

Old Dominion University

## ODU Digital Commons

---

Electrical & Computer Engineering Theses & Dissertations

Electrical & Computer Engineering

---

Spring 2002

# Improvements in Wavelength Modulation Spectroscopy Using Ratios of Higher Harmonics

James Michael Barrington  
*Old Dominion University*

Follow this and additional works at: [https://digitalcommons.odu.edu/ece\\_etds](https://digitalcommons.odu.edu/ece_etds)



Part of the [Electrical and Computer Engineering Commons](#), [Engineering Physics Commons](#), and the [Materials Science and Engineering Commons](#)

---

### Recommended Citation

Barrington, James M.. "Improvements in Wavelength Modulation Spectroscopy Using Ratios of Higher Harmonics" (2002). Master of Science (MS), Thesis, Electrical & Computer Engineering, Old Dominion University, DOI: 10.25777/wmq5-5h59  
[https://digitalcommons.odu.edu/ece\\_etds/292](https://digitalcommons.odu.edu/ece_etds/292)

This Thesis is brought to you for free and open access by the Electrical & Computer Engineering at ODU Digital Commons. It has been accepted for inclusion in Electrical & Computer Engineering Theses & Dissertations by an authorized administrator of ODU Digital Commons. For more information, please contact [digitalcommons@odu.edu](mailto:digitalcommons@odu.edu).

**IMPROVEMENTS IN WAVELENGTH MODULATION  
SPECTROSCOPY USING RATIOS OF HIGHER HARMONICS**

by

James Michael Barrington  
B.S. May 2000, Old Dominion University

A Thesis Submitted to the Faculty of  
Old Dominion University in Partial Fulfillment of the  
Requirement for the Degree of

MASTER OF SCIENCE

ELECTRICAL ENGINEERING

OLD DOMINION UNIVERSITY  
May 2002

Approved by:

---

Amin N. Dharamsi (Director)

---

Ravindra P. Joshi (Member)

---

Karl H. Schoenbach (Member)

## **ABSTRACT**

### **IMPROVEMENTS IN WAVELENGTH MODULATION SPECTROSCOPY USING RATIOS OF HIGHER HARMONICS**

James Michael Barrington  
Old Dominion University, 2002  
Director: Dr. Amin N. Dharamsi

Experiments in Wavelength Modulation Spectroscopy have been conducted at Old Dominion University since 1996. The method provides a highly sensitive, non-intrusive method of probing gases. Research has concentrated on effectively modeling the higher harmonic shapes that are measured experimentally. Accurately modeling these signals will result in the ability to reliably extract the information contained in transition line shapes.

In order to accurately depict the signals, the theory must be thoroughly understood. This thesis develops the theory of Wavelength Modulation Spectroscopy from two aspects: a direct Fourier series expansion of a time varying intensity profile and through communication theory. In addition, a method of ratioing higher harmonics is introduced. This method reduces the subjectivity in modeling and will eventually lead to future automation.

## ACKNOWLEDGMENTS

I will be eternally grateful to a fine advisor, exceptional teacher, and special friend, Dr. Amin Dharamsi. His unremitting patience and thoughtful guidance allowed me to thoroughly comprehend this project instead of just polishing its veneer. The mathematical maturity, physics knowledge, and programming skills I obtained in this research will undoubtedly help me throughout my engineering career. Additionally, I would like to thank the Electrical and Computer Engineering Faculty at Old Dominion University and the Engineering Department at Tidewater Community College for providing me with the engineering background to pursue this research and Dr. Audra Bullock for giving this project a firm foundation to build on.

I would not have been able to continue with school without the financial support from the Virginia Space Grant Consortium for the Undergraduate Program, the GI Bill Educational Benefits, and the Graduate Assistance in Areas of National Need (GAANN) doctoral fellowship.

Finally, I would like to thank my family for allowing me to pursue this formal education and for providing me a constant education in life; my son, Josh, who keeps me young; and my daughter, Manda, who reminds me to live; and Deloyce, my best friend, who teaches me to love.



## TABLE OF CONTENTS

	Page
LIST OF FIGURES .....	v
LIST OF TABLES .....	viii
INTRODUCTION .....	1
1.1 Basic Theory .....	2
DETAILED THEORY .....	10
2.1 Fourier Series Expansion of the Detected Intensity Signal .....	10
2.2 Derivation using Communication Theory .....	16
ABSORPTION PROFILES .....	30
3.1 Doppler Profile .....	30
3.2 The Lorentzian Profile .....	33
3.3 Voigt Profile .....	36
3.4 Profile Narrowing .....	37
EXPERIMENTAL DATA .....	40
4.1 Ratioing Harmonic Information .....	40
4.2 Pressure vs. Harmonic Curves .....	47
4.3 Modeling several lines with a single ramp .....	54
FUTURE WORK .....	57
REFERENCES .....	59
APPENDIX .....	60
VITA .....	78

## LIST OF FIGURES

Figure	Page
1-1 An absorption spectrum of an arbitrary molecule showing four absorption profiles.....	3
1-2a Direct absorption experiment setup using a tunable laser.....	4
1-2b Direct absorption achieved by sweeping a laser. Upper graph shows four absorption profiles. Lower graph depicts the resulting intensity profile.....	5
1-3 Upper figure shows the laser tuned off to the left side of an absorption profile. The middle figure shows the effect of the modulation on the lasers frequency. The lower graph presents the time domain signal of the detected intensity over two oscillations of modulation. ....	5
1-4 A Fourier series expansion of a single cycle of an AC coupled intensity signal, blue.....	6
1-5 Upper figure shows the laser tuned off to the left side of an absorption profile. The middle figure shows the effect of the modulation on the lasers frequency. The lower graph presents the time domain signal of the detected intensity over two oscillations of modulation.....	7
1-6 Upper figure shows the laser tuned to the center of an absorption profile. The middle figure shows the effect of the modulation on the lasers frequency. The lower graph presents the time domain signal of the detected intensity over two oscillations of modulation.....	8
1-7 N1 through N4 Fourier coefficient variations as ramp is used to sweep the center frequency of the modulation across an absorption line.....	8
2-1 Sideband magnitude plot of a modulation index of 5.....	21
2-2 Angle information positive frequency sidebands.....	22
2-3 Angle information negative frequency sidebands.....	22
2-4 DC signal generation with no absorption line.....	23
2-5 N1 equals zero in the absence of an absorption line.....	24
2-6 N2 equals zero in the absence of an absorption line.....	25

2-7 N3 equals zero in the absence of an absorption line.....	26
2-8 Effective laser profiles for N1 though N8.....	28
4-1 Experimental Setup.....	41
4-2 N2 and N8 harmonic signals of RQ (7,8) measured at 154 cm. Calculated models are shown in red and data shown in blue. Calculated line width is .0505 cm <sup>-1</sup> and line strength is 8.78 cm/mol.....	44
4-3 N2 and N8 harmonic signals of RQ (7,8) measured at 3219 cm. Calculated models are shown in red and data shown in blue. Calculated line width is .0505 cm <sup>-1</sup> and line strength is 8.78 cm/mol.....	45
4-4 N2 and N8 harmonic signals of RQ (7,8) measured at 5279 cm. Calculated models are shown in red and data shown in blue. Calculated line width is .0505 cm <sup>-1</sup> and line strength is 8.78 cm/mol.....	46
4-5 Theoretical Even Harmonic Magnitudes vs. Pressure for a Gaussian Line shape.....	48
4-6 Direct absorption of RQ(7,8) at 50, 500, 1000, and 1500 torr.....	49
4-7 N2 Line center Magnitude vs. pressure for RQ(7,8) in oxygen. Modeled as a Voigt with a line width of 0.0487 cm <sup>-1</sup> .....	50
4-8 N4 Line center Magnitude vs. pressure for RQ(7,8) in oxygen. Modeled as a Voigt with a line width of 0.0487 cm <sup>-1</sup> .....	50
4-9 N6 Line center Magnitude vs. pressure for RQ(7,8) in oxygen. Modeled as a Voigt with a line width of 0.0487 cm <sup>-1</sup> .....	51
4-10 N8 Line center Magnitude vs. pressure for RQ(7,8) in oxygen. Modeled as a Voigt with a line width of 0.0487 cm <sup>-1</sup> .....	51
4-11 Profiles for N1 through N8 for RQ(7,8) at 500 torr.....	52
4-12 Reside vs. Harmonic order for the comparison of a Voigt model of RQ(7,8) with a line width of 0.0487 cm <sup>-1</sup> and line strength of 8.13 cm/mol from 50 torr to 1602 torr.....	53
4-13 Direct absorption of RR(13,13), RR(13,13), RR(43,43), and RQ(12,13).....	55

4-14	N2 profile for RR(13,13), RR(13,13), RR(43,43), and RQ(12,13).....	55
4-15	N7 profile for RR(13,13), RR(13,13), RR(43,43), and RQ(12,13).....	56
4-16	N8 profile for RR(13,13), RR(13,13), RR(43,43), and RQ(12,13).....	56
A-1	Top left panel displays the absorption profile. The second panel on the left is the laser profile. The third panel is the Fourier Transform of the detected intensity. The bottom panel is selectable between the harmonic phase angles or the time domain signal. The right panels show the magnitudes of N1 through N4.....	60



## LIST OF TABLES

Table	Page
4-1 Comparison of experimental calculations and HITRAN data.....	54

# CHAPTER I

## INTRODUCTION

Accurately measuring the line shape of an electron transition in a gaseous medium can result in precise measurements of molecular density, temperature, and pressure. In addition, it can provide insight to the basic physics of the system, such as molecular collision parameters. However, obtaining a precise line shape measurement is not easy. Conventional Absorption spectroscopy has been used for over one hundred years to identify molecular species; however, its ability to measure the line shape of a single transition is severely limited by the precision of its dispersion device. One interesting and useful variant of absorption spectroscopy is Wavelength Modulation Absorption Spectroscopy (WMS)<sup>1,2</sup>. This method uses several fundamental engineering principles, such as frequency modulation and Fourier series expansion, to increase the signal to noise ratio.

The primary advantage of WMS is that it can provide a precise measurement of an absorption feature with limited equipment, lending it to field use. Since all the information about a transition resides in the line shape function, the method is a powerful tool for mining such information. However, a complete understanding of this method is required to exploit its results. Current applications overlook the information inherent in the higher harmonics. This thesis develops the theory of WMS and the advantages of higher harmonic detection.

The journal model for this thesis is *Journal of Applied Physics*.



## 1.1 Basic Theory

This section discusses the fundamentals of WMS in a qualitative manner and is added to provide an intuitive explanation of the method. A more rigorous development of each step of the experiment will be provided in later chapters.

Absorption spectroscopy has been used for over one hundred years to identify molecular species. A simple example of absorption spectroscopy is a molecule that only contains two energy levels,  $E_1$  and  $E_2$ , in which an electron can exist. If an electron starts in the lower level, the only way for it to transition to the upper level is to add the energy equal to the difference between the levels. This can be accomplished by absorption of a photon at the correct color or frequency,  $E_2 - E_1 = E = h\nu$ , where  $h$  is Planck's constant and  $\nu$  is frequency of light. Therefore, passing white light through a medium and then separating the spectrum by using a prism or diffraction grating, the presence of this simplified molecule can be identified by the dark or dim line at the frequency that corresponds to the appropriate energy. This is the procedure for conventional Absorption Spectroscopy. Figure 1 is a simple example of this experiment showing four absorption lines of an arbitrary molecule. However, in real molecules there are numerous energy levels with their separations controlled by complex bounding schemes, which results in a unique signature for each molecule.

Additionally, figure 1-1 shows that an absorption line is not at a single frequency, i.e., note that the absorption lines do not have well defined edges. This is because absorption lines are not delta functions but are distributed over a frequency region. Primarily, this distribution is a result of collisions and Doppler shifts in a gaseous

medium. Embedded in this distribution is information about the system. For example, the magnitude of the Doppler shift a molecule can experience depends on its kinetic energy, which is dependent on temperature; e.g., the distribution of absorbed frequencies

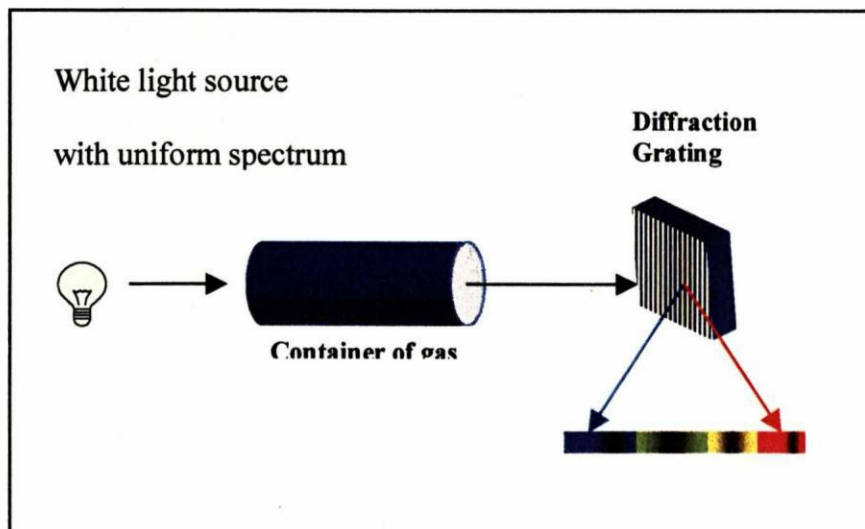


**Fig. 1-1 An absorption spectrum of an arbitrary molecule showing four absorption profiles.**

is smaller at lower temperatures. Therefore, a precise measurement of the absorption profile, frequency versus magnitude, will allow for the extraction of this information. In order to obtain this information using the equipment in figure 1-1, a light source with a uniform distribution across the spectrum and a high resolution diffraction grating or prism would be required. However, a much simpler and less expensive experimental setup reverses the resolution of the source and the detector. In this case, a tunable light source, laser, is detected by a photodiode with a flat response in the frequency range of concern, see figure 1-2a. In order for this to work, the laser linewidth has to be much smaller than the absorption feature to be probed, i.e., the laser profile should be essentially a delta function in comparison to the absorption profile. Therefore, as the laser is tuned across the absorption feature, the intensity variation is a direct

representation of the absorption profile, as shown in figure 1-2b. Although the equipment has changed, this is still simply Absorption Spectroscopy. Unfortunately, the precision of this method is limited by noise. For example, light from any other source with a frequency within the spectrum of the detector's bandwidth will also be detected. The easiest way around this is to provide the laser signal with a unique time domain signature of its own allowing its intensity to be identified and separated from other sources, thus, the wavelength modulation.

Wavelength modulation is spectroscopy's counterpart to frequency modulation techniques used in communications engineering. The frequency of the carrier is proportional to the magnitude of the modulation signal, and the desired unique signature is provided by the frequency characteristics of the modulation signal. For example, if the laser is modulated with a sinusoid, the frequency of the laser will oscillate sinusoidally at the frequency of the modulation, with the magnitude of the frequency variation controlled by the magnitude of the modulating sine wave. It is important to note that in the absence of absorption, the detector is oblivious to this modulation, i.e., the detector is only sensitive to intensity variations, not frequency variations.

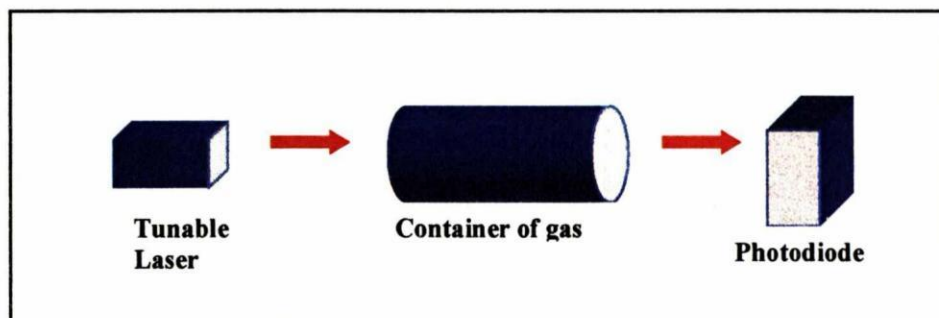


**Fig. 1-2a Direct absorption experiment setup using a tunable laser.**



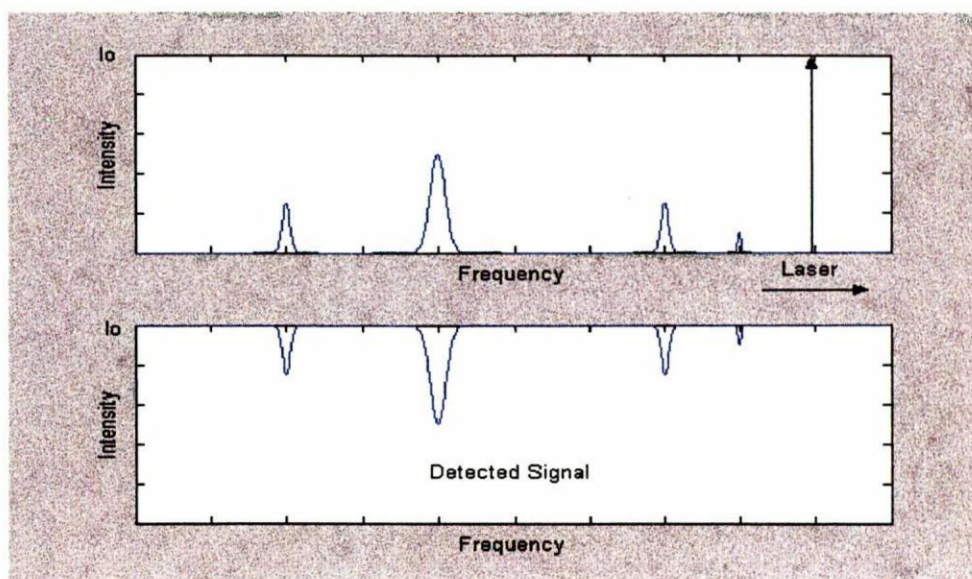


**Fig. 1-2b** Direct absorption achieved by sweeping a laser. Upper graph shows four absorption profiles. Lower graph depicts the resulting intensity profile.

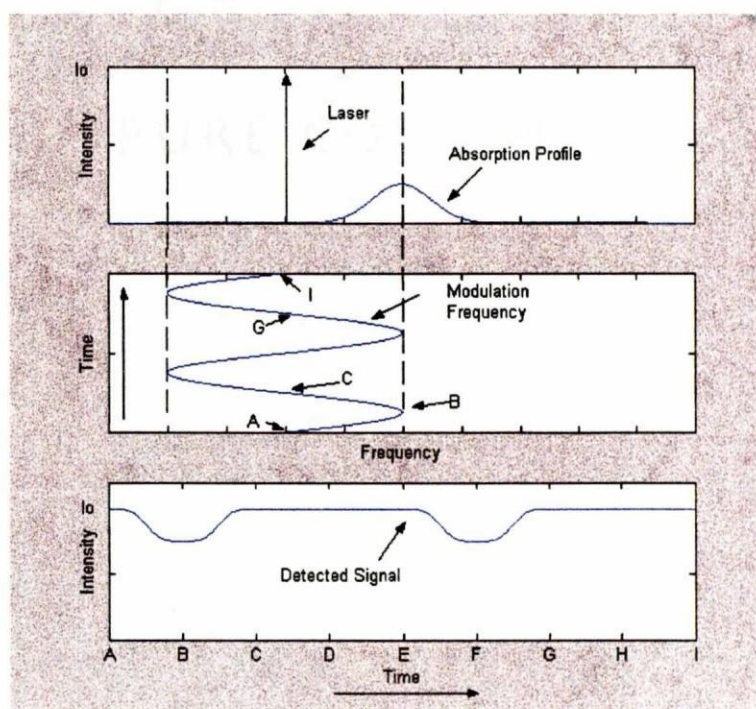
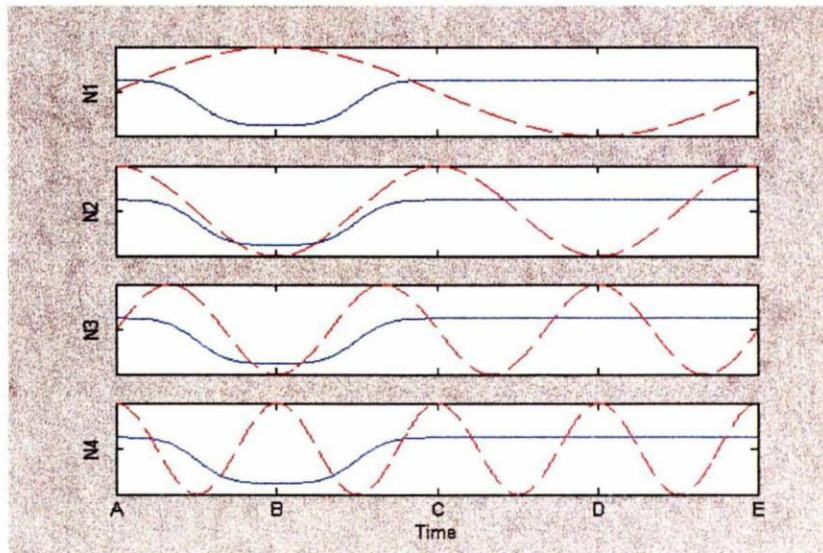


**Fig. 1-3** Upper figure shows the laser tuned off to the left side of an absorption profile. The middle figure shows the effect of the modulation on the laser's frequency. The lower graph presents the time domain signal of the detected intensity over two oscillations of modulation.

However, in the presence of absorption, the absorption profile is sinusoidally sampled resulting in the detector's intensity to vary at a frequency proportional to that of the modulation. Now the light emitting from the laser has a unique signature that can be extracted from the detector. Figure 1-3 shows the intensity variations over two cycles of modulation with laser initially tuned to the left of the absorption line. Although the modulation has provided a method to separate the signal from the noise, the absorption line is now encoded in a nonlinear sample and can no longer be directly extracted. However, any periodic function can be expanded using a Fourier series, i.e., equating the signal to a summation of sinusoidal waves at harmonics of the fundamental frequency;

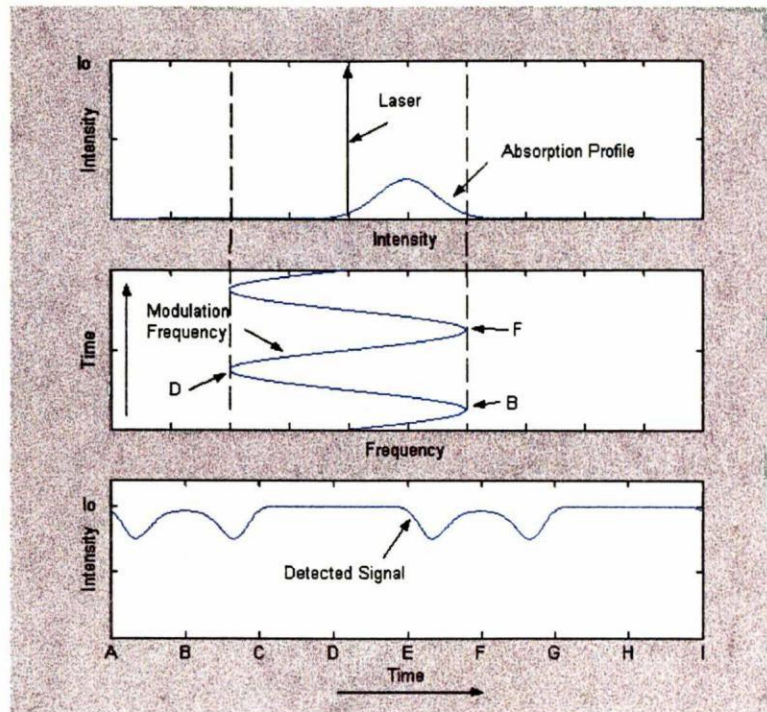
$$f(t) = A_0 + \sum_{k=1}^{\infty} A_k \cos(k\omega_0 t) + B_k \sin(k\omega_0 t), \quad (1.1)$$

where  $A_0$  is the DC signal and  $\omega_0$  is the fundamental frequency, or the modulation frequency in this instance. The coefficients,  $A_k$  and  $B_k$ , indicate the contribution of each harmonic to the composite signal.



**Fig. 1-4** A Fourier series expansion of a single cycle of an AC coupled intensity signal, blue.

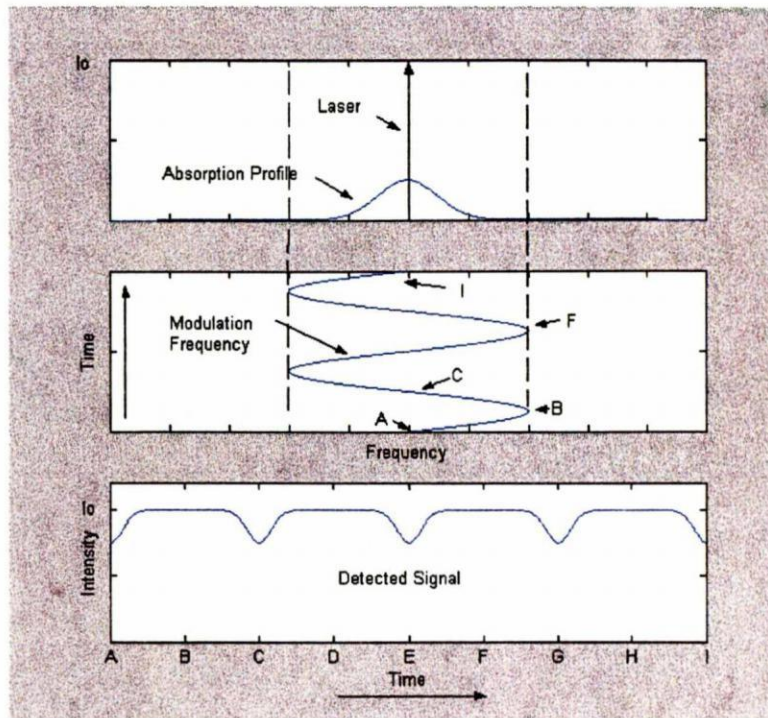




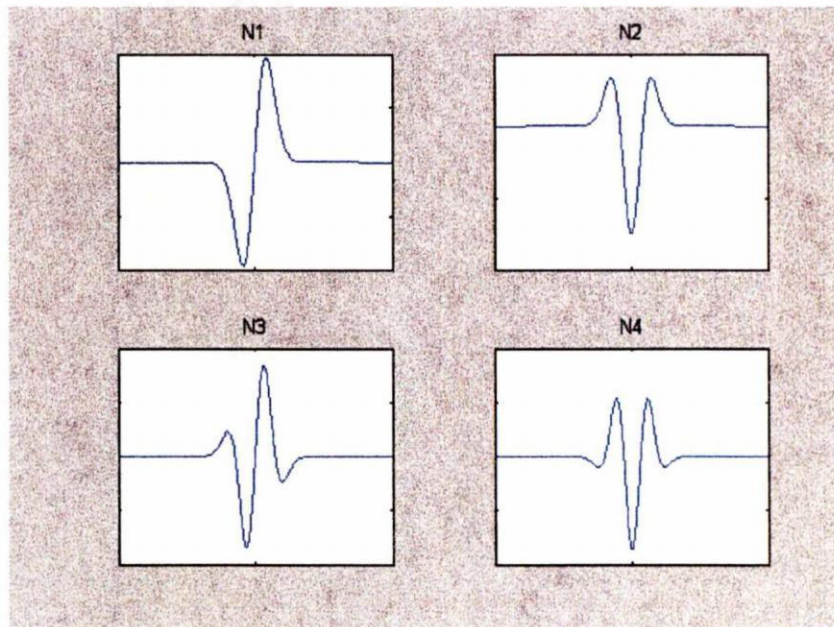
**Fig. 1-5** Upper figure shows the laser tuned off to the left side of an absorption profile. The middle figure shows the effect of the modulation on the laser's frequency. The lower graph presents the time domain signal of the detected intensity over two oscillations of modulation.

Figure 1-4 graphically shows the first step of a Fourier series coefficient calculation for the first four harmonics of the AC coupled intensity variations detected when the center of the modulation is to the left of the absorption line. One cycle of the intensity variation is multiplied with the sine/cosine of the harmonic signals and summed to determine their coefficients. Note that the odd harmonic signals are expanded with a sine wave and the even harmonic signals are expanded with a cosine function, resulting in a  $90^\circ$  difference. When the modulation is combined with sweeping of the center frequency, the harmonic coefficients vary accordingly. Figures 1-5 and 1-6 show the intensity variations at two other laser center frequencies, slightly to the left of the absorption profile and centered on the profile respectively.





**Fig. 1-6** Upper figure shows the laser tuned to the center of an absorption profile. The middle figure shows the effect of the modulation on the laser's frequency. The lower graph presents the time domain signal of the detected intensity over two oscillations of modulation.



**Fig. 1-7** N1 through N4 Fourier coefficient variations as ramp is used to sweep the center frequency of the modulation across an absorption line.

Figure 1-7 shows the variation of the first four Fourier expansion coefficients as the laser is swept across an absorption line. Therefore, WMS is simply a Fourier series expansion of a sinusoidal sampled absorption profile. Although its concept is simple, the technique of analyzing higher harmonics is underutilized and generally not well understood. The strengths of this method will be developed further in the detailed theory section.

## CHAPTER II

### DETAILED THEORY

Chapter two develops the theory of wavelength modulation from two different aspects: a method based on laser intensity directly sampling an absorption feature and a model based on communication sidebands. Both methods require the modulation of a light source's frequency. There are several ways this can be achieved. For example, a diode laser can be phase modulated using the Kerr effect<sup>3</sup> or frequency modulated using the drive current. However, the overall goal of this project is to develop a reliable, portable and cost effective means of making precise measurements of absorption profiles. Therefore, most discussions are directed towards frequency modulation through drive current.

#### 2.1 Fourier Series Expansion of the Detected Intensity Signal

This method, developed by Wilson<sup>4</sup>, was introduced in chapter one. An absorption shape is sampled with a delta function whose frequency has a sinusoidal variation; then the intensity variation is expanded with a Fourier series. The harmonic coefficients versus the laser's unmodulated center frequency are the resulting signals. This section will discuss this method more rigorously.

Unfortunately, the first step in this procedure is an approximation. As stated above, the absorption profile is sampled by a delta function. In WMS, the absorption profile is probed with a laser; therefore, the laser profile is considered a delta function. This approximation is acceptable if the absorption profile is much wider than the laser linewidth. However, if necessary, the laser linewidth can be incorporated, as is done at




the end of this section. While this refinement of the theory comes at a significant computational expense, it is shown that the results obtained by using the delta function approximation do not introduce any uncertainty in the results, within the experimental precision of this work.

The absorption of light in a weakly absorbing medium is defined by the Beer-Lambert Law<sup>5</sup>,

$$I = I_0 e^{-\alpha(\omega)L}, \quad (2.1)$$

where  $\alpha(\omega)$  is the angular frequency dependent absorption coefficient, an absorption line,  $L$  is the path length,  $I_0$  is the initial intensity, and  $I$  is the detected intensity. The initial intensity in this case is that of a frequency modulated diode laser. As stated above, the simplest and most inexpensive method of modulating a diode laser's frequency is through its drive current. Theoretically, as the current is modulated, the temperature varies in the laser resulting in the variation of the laser cavity's physical dimensions as it dissipates the heat. An increase in current results in an increase in cavity size and wavelength. In addition, there is an expected phase difference,  $\theta$ , between the modulation current and the cavity variations due to the specific heat and mass of the semiconductor material. However, using the drive current to tune the laser also varies the intensity, i.e., an increase in current increases the generation of electron hole pairs, linearly increasing the radiative recombination, thus intensity. Therefore, the instantaneous intensity and frequency of a diode laser signal with no linewidth that is modulated with a sine wave is

$$I(\omega, t) = (I_0 + k_I A \sin(\omega_m t + \phi)) \delta(\omega_L - k_f A \sin(\omega_m t + \theta)), \quad (2.2)$$


  
**Intensity Modulation      Wavelength Modulation**

where  $\omega_L$  is the laser center frequency without modulation,  $\omega_m$  is the modulation frequency,  $\phi$  is the phase difference between the drive current and the intensity modulation, and  $A$  is the amplitude of the drive signal applied to the current driver in volts. Two other constants are incorporated in this equation: the constant of proportionality between the drive voltage and the intensity,  $k_I$ , and constant of proportionality between the drive voltage and the frequency,  $k_f$ . Both of these values can easily be obtained experimentally by applying a linear ramp to the drive current and determining the slope of the intensity and frequency variations. Finally, to determine the detected time varying intensity signal, the laser signal is integrated over frequency with the absorption profile as describe by the Beer-Lambert law,

$$I_D(t) = \int_{-\infty}^{\infty} (I_0 + k_I A \sin(\omega_m t + \phi)) \delta(\omega_L - k_f A \sin(\omega_m t + \theta)) * e^{-\alpha(\omega)L} d\omega. \quad (2.3)$$

This simply results in

$$I_D(t) = (I_0 + k_I A \sin(\omega_m t + \phi)) * e^{-\alpha(\omega_L + k_f A \sin \omega_m t + \theta)L}. \quad (2.4)$$

Next, a Fourier series expansion is conducted on the time varying intensity signal,

$$f(t) = A_0 + \sum_{N=1}^{\infty} A_N \cos(N\omega_0 t) + B_N \sin(N\omega_0 t), \quad (2.5)$$

$$N = 1, 2, 3, 4, \dots$$

where  $A_0$  is the DC offset and the harmonic coefficients are calculated using

$$A_N = \frac{1}{T} \int_0^T [(I_0 + k_I A \sin(\omega_m t + \phi)) * e^{-\alpha(\omega_L - k_f A \sin(\omega_m t + \theta))L}] \cos(N\omega_m t) dt, \text{ and} \quad (2.6)$$

$$B_N = \frac{1}{T} \int_0^T [(I_0 + k_I A \sin(\omega_m t + \phi)) * e^{-\alpha(\omega_L - k_f A \sin(\omega_m t + \theta))L}] \sin(N\omega_m t) dt. \quad (2.7)$$

These equations can be broken into two distinct sections, pure wavelength modulation spectroscopy and distortions due to intensity variations. For example, the pure frequency modulation is described by

$$A_{N_f} = \frac{1}{T} \int_0^T [I_0 * e^{-\alpha(\omega_L - k_f A \sin(\omega_m t + \theta))L}] \cos(N\omega_m t) dt, \text{ and} \quad (2.8)$$

$$B_{N_f} = \frac{1}{T} \int_0^T [I_0 * e^{-\alpha(\omega_L - k_f A \sin(\omega_m t + \theta))L}] \sin(N\omega_m t) dt. \quad (2.9)$$

Similarly, the Fourier components describing the effect of intensity variations are given by

$$A_{N_I} = \frac{1}{T} \int_0^T [(k_I B \sin(\omega_m t + \phi)) * e^{-\alpha(\omega_L - k_f A \sin(\omega_m t + \theta))L}] \cos(N\omega_m t) dt, \text{ and} \quad (2.10)$$

$$B_{N_I} = \frac{1}{T} \int_0^T [(k_I A \sin(\omega_m t + \phi)) * e^{-\alpha(\omega_L - k_f A \sin(\omega_m t + \theta))L}] \sin(N\omega_m t) dt. \quad (2.11)$$

If a modulation method other than drive current is selected, i.e., angle modulation via a Pockels cell<sup>5</sup>, then the formulas for pure wavelength modulation could be used.

It is important to note that these equations provide a single set of coefficients, i.e., a ramp has not been included to allow for sweeping the center frequency. Therefore, these values calculated are assigned to the unmodulated laser center frequency. However, before adding a ramp to sweep the center frequency of the modulation, it is important to note several simple phenomena inherent to wavelength modulation. First, consider the special case of no absorption. In the absence of absorption, equations 6 and 7 simplify to

$$A_N = \frac{1}{T} \int_0^T [(I_0 + k_I A \sin(\omega_m t + \phi))] \cos(N\omega_m t) dt = \frac{1}{T} \int_0^T k_I A \sin(\omega_m t + \phi) \cos(N\omega_m t) dt,$$



$$A_1 = \frac{1}{T} \int_0^T k_I A \sin(\omega_m t + \phi) \cos(\omega_m t) dt, \text{ and} \quad (2.12)$$

$$B_N = \frac{1}{T} \int_0^T [(I_0 + k_I A \sin(\omega_m t + \phi))] \sin(N\omega_m t) dt = \frac{1}{T} \int_0^T k_I A \sin(\omega_m t + \phi) \sin(N\omega_m t) dt,$$

$$B_1 = \frac{1}{T} \int_0^T k_I A \sin(\omega_m t + \phi) \sin(\omega_m t) dt \quad (2.13)$$

Therefore, only a first harmonic coefficient is present. This results in an offset of the first harmonic signal.

Next, consider the case presented in figure 1-3, i.e., the laser is tuned left of the absorption line. However, for a portion of the modulation the laser's center frequency is interacting with the absorption line resulting in a periodic signal. Therefore, when the Fourier coefficients are calculated, each harmonic is assigned a value on the unmodulated laser's center frequency. This is the source of modulation broadening.

Finally, phase differences between harmonics should be addressed. This method is based on the Fourier expansion of a periodic intensity signal. Experimentally, this is accomplished with a lock-in-amplifier (LIA)<sup>6</sup>. Basically, the LIA provides phase sensitive detection of periodic signals by comparing the detected signal to a replica of the modulation signal. A sync signal from the oscillator that creates the modulation signal is sent to the LIA. The sync signal is normally a square wave, which indicates the zero crossings and polarity of the modulation sine wave. The LIA creates tunable phase, unit magnitude quadrature components, X and Y, at the frequency or a harmonic of the sync signal. It then multiplies the components with the input signal. The product of the X component and the input provides Fourier coefficient for the respective harmonic that is in phase with the modulation signal. The product of the Y component and the input

indicates provides Fourier coefficient for the respective harmonic that is  $90^\circ$  out of phase with the modulation signal. Normally, using a variable delay, the quadrature components are tuned to maximize the X component and minimize the Y component, i.e., set the phase difference between the modulation input and actual frequency modulation,  $\theta$ , to zero. Additionally, at small frequencies, there is not a phase difference between the intensity modulation and the modulation signal, thus  $\phi$  equals 0. Consequently, the sine coefficient for the first harmonic can be rewritten as

$$B_1 = \frac{1}{T} \int_0^T \left[ (I_0 + k_I A \sin(\omega_m t)) * e^{-\alpha(\omega_L - k_f A \sin(\omega_m t + \theta))L} \right] \sin(\omega_m t + \theta_1) dt. \quad (2.14)$$

For the second harmonic, the time delay that created the phase difference between the modulation input and the actual frequency modulation has not changed, but the frequency that it is compared to has doubled. Therefore, the phase difference must be twice that of the first harmonic. In addition, the second harmonic is an even signal where the first harmonic is odd. Therefore, the LIA to Fourier coefficients calculated by the LIA can be described by

$$B_N = \frac{1}{T} \int_0^T \left[ (I_0 + k_I A \sin(\omega_m t)) * e^{-\alpha(\omega_L - k_f A \sin(\omega_m t + \theta))L} \right] \sin(N\omega_m t + \theta_{LIA}) dt, \quad (2.15)$$

$$\text{where } \theta_{LIA} = N\theta_1 + 90 \bmod((N+1), 2). \quad (2.16)$$

Finally, to allow for sweeping of the laser, a ramp is superimposed onto the modulation,

$$I(\omega, t) = \underbrace{(I_0 + k_I (R't + A \sin(\omega_m t + \phi)))}_{\text{Intensity Modulation}} \underbrace{\delta(\omega_L + k_f (R't - A \sin(\omega_m t + \theta)))}_{\text{Wavelength Modulation}}, \quad (2.17)$$

where  $R'$  is the slope of the ramp. This signal can easily be added to equation 2.3.

However, for ease of calculation, the ramp is normally consider in steps,

$$I(\omega, t) = (I_0 + I_s n + k_I B \sin(\omega_m t + \phi)) \delta(\omega_L + \omega_s n - k_f A \sin(\omega_m t + \theta)), \quad (2.18)$$

where  $n = 0, 1, 2, 3, 4 \dots$

and the  $I_s$  and  $\omega_s$  are steps in intensity and angular frequency, respectively. The slope of the ramp must be significantly smaller than that of the modulation to avoid distortion.

Inclusion of laser line shape is actually quite simple mathematically. The laser line shape replaces the delta function in equation 2.2,

$$I(\omega, t) = (I_0 + k_I B \sin(\omega_m t + \phi)) g(\omega_L - k_f A \sin(\omega_m t + \theta)). \quad (2.19)$$

Unfortunately, the exclusion of the delta function requires significantly more calculations. For example, just one step of the modulation requires numerous calculations of the absorption profile to be weighted by the laser profile,

$$I_D(t) = \int_{-\infty}^{\infty} (I_0 + k_I B \sin(\omega_m t + \phi)) g(\omega_L - k_f A \sin(\omega_m t + \theta)) * e^{-\alpha(\omega)L} d\omega; \quad (2.20)$$

however, this has been done in MATLAB with idealized values to validate the theory.

## 2.2 Derivation using Communication Theory

The last section described wavelength modulation spectroscopy as a Fourier series expansion of time varying intensity field. In the derivation, the intensity of the laser was treated as a delta function, which sampled the absorption profile. It ignored the e-field sidebands normally associated with frequency modulation in communication theory. Although this formulation adequately describes WMS due to the number of the sidebands



that interact with the absorption feature, it cannot be extended to Frequency Modulation Absorption Spectroscopy<sup>7</sup>, which has a modulation frequency larger than width of the absorption feature. Therefore, as a matter of completeness, this section derives WMS in the frequency domain using e-fields.

In the frequency domain, the modulated laser is represented by numerous sidebands spaced by the modulation frequency whose magnitudes are controlled by Bessel functions. When these sidebands interact with an absorption feature, intensity modulations at harmonics of the modulation frequency can be detected with a photodiode.

Also in this method, to make the mathematics tractable, the linewidth of the laser is approximated as a delta function in the frequency domain<sup>8</sup>, or a sinusoidal wave in the time domain,

$$A = \cos(\omega_L t), \quad (2.21)$$

where  $\omega_L$  is the laser angular frequency and  $t$  is time. When the laser is frequency modulated by a sine wave, its instantaneous frequency<sup>9</sup> is defined as

$$\omega_i = \omega_L - k_f V(t) = \omega_L - k_f A \sin(\omega_m t + \phi), \quad (2.22)$$

where  $\omega_m$  is the modulation frequency,  $A$  is the amplitude of the sinusoidal signal and  $\phi$  is the phase difference between the modulation signal and the actual modulation. As discussed in section 2.1, the modulation signal applied to a laser diode drive current manifests itself in two ways, frequency and intensity modulation; however, before addressing intensity variations, frequency modulation is derived first. Integrating equation 2.21 to find the phase results in

$$\theta(t) = \int_{-\infty}^t \omega_i dt = \int_{-\infty}^t \omega_L - kA \sin(\omega_m t + \phi) dt = \omega_L t + \theta + \left( \frac{\beta}{\omega_m} \right) \cos(\omega_m t + \phi), \quad (2.23)$$

where  $\beta = k_f A$  and  $\beta/\omega_m$  is referred to as the modulation index in communication theory.

Assuming the signal starts with a zero phase, i.e., setting  $\theta$  equal to 0, the pure wavelength modulation laser signal is defined as

$$E_0 \cos\left(\omega_L t + \frac{\beta}{\omega_m} \cos(\omega_m t + \phi)\right). \quad (2.24)$$

In order to have a better understanding of the signal spectrum of this compact formula, it is instructive to expand it into its frequency components. Expanding this signal using trigonometric and Bessel function identities results in

$$\begin{aligned} E_0 \cos\left(\omega_L t + \frac{\beta}{\omega_m} \cos(\omega_m t + \phi)\right) \\ = E_0 \cos(\omega_L t) \left( \frac{\beta}{\omega_m} \right) \cos(\omega_m t + \phi) - E_0 \sin(\omega_L t) \left( \frac{\beta}{\omega_m} \right) \sin(\omega_m t + \phi), \end{aligned} \quad (2.25)$$

$$\begin{aligned} = E_0 \cos(\omega_L t) \left( J_0\left(\frac{\beta}{\omega_m}\right) + 2 \sum_{n=1}^{\infty} (-1)^n J_{2n}\left(\frac{\beta}{\omega_m}\right) \cos(2n(\omega_m t + \phi)) \right) - \\ E_0 \sin(\omega_L t) \left( 2 \sum_{n=1}^{\infty} (-1)^{n+1} J_{2n-1}\left(\frac{\beta}{\omega_m}\right) \cos((2n-1)(\omega_m t + \phi)) \right), \end{aligned} \quad (2.26)$$

where  $n=0, 1, 2, 3, \dots$

Further expanding the first part of the equation

$$\begin{aligned}
 E_0 \cos(\omega_L t) & \left( J_0\left(\frac{\beta}{\omega_m}\right) + 2 \sum_{n=1}^{\infty} (-1)^n J_{2n}\left(\frac{\beta}{\omega_m}\right) \cos(2n(\omega_m t + \phi)) \right) \\
 & = E_0 J_0\left(\frac{\beta}{\omega_m}\right) \cos(\omega_L t) + E_0 2 \sum_{n=1}^{\infty} (-1)^n J_{2n}\left(\frac{\beta}{\omega_m}\right) [\cos(\omega_L t + 2n(\omega_m t + \phi)) + \\
 & \quad \cos(\omega_L t - 2n(\omega_m t + \phi))], \tag{2.27}
 \end{aligned}$$

$$\begin{aligned}
 & = E_0 \sum_{n=-\infty}^{\infty} \cos(n\pi) J_{2n}\left(\frac{\beta}{\omega_m}\right) \cos(\omega_L t + 2n(\omega_m t + \phi)) \\
 & = E_0 \sum_{n=-\infty}^{\infty} J_{2n}\left(\frac{\beta}{\omega_m}\right) \cos(\omega_L t + 2n(\omega_m t + \phi) + n\pi) \\
 & = E_0 \sum_{n=-\infty}^{\infty} J_{2n}\left(\frac{\beta}{\omega_m}\right) \cos\left(\omega_L t + 2n(\omega_m t + \phi) + \frac{\pi}{2}\right). \tag{2.28}
 \end{aligned}$$

Expanding the second part of the equation

$$\begin{aligned}
 & - E_0 \sin(\omega_L t) \left( 2 \sum_{n=1}^{\infty} (-1)^{n+1} J_{2n-1}\left(\frac{\beta}{\omega_m}\right) \cos((2n-1)(\omega_m t + \phi)) \right) \\
 & = E_0 \sum_{n=1}^{\infty} (-1)^n J_{2n-1}\left(\frac{\beta}{\omega_m}\right) [\sin(\omega_L t + (2n-1)(\omega_m t + \phi)) + \\
 & \quad \sin(\omega_L t - (2n-1)(\omega_m t + \phi))] , \tag{2.29}
 \end{aligned}$$



$$\begin{aligned}
&= E_0 \sum_{n=1}^{\infty} J_{2n-1} \left( \frac{\beta}{\omega_m} \right) \left[ \cos \left( \omega_L t + (2n-1)(\omega_m t + \phi) + n\pi - \frac{\pi}{2} \right) + \right. \\
&\quad \left. \cos \left( \omega_L t - (2n-1)(\omega_m t + \phi) + n\pi - \frac{\pi}{2} \right) \right], \quad (2.30)
\end{aligned}$$

$$\begin{aligned}
&= E_0 \sum_{n=1}^{\infty} J_{2n-1} \left( \frac{\beta}{\omega_m} \right) \left[ \cos \left( \omega_L t + (2n-1)(\omega_m t + \phi + \frac{\pi}{2}) \right) + \right. \\
&\quad \left. \cos \left( \omega_L t - (2n-1)(\omega_m t + \phi + \frac{\pi}{2}) \right) \right]. \quad (2.31)
\end{aligned}$$

Recombining the equations results in another compact equation, which explicitly shows the frequency components and phases from the modulation<sup>9</sup>,

$$E(t) = E_0 \sum_{n=-\infty}^{\infty} J_n \left( \frac{\beta}{\omega_m} \right) \cos \left( \omega_L t + n(\omega_m t + \phi + \frac{\pi}{2}) \right). \quad (2.32)$$

Although classically the e-field is what interacts with the absorption feature, optical detectors (eyes, photographic emulsions, and photoelectric devices) respond to radiation intensity; therefore, the Poynting vector of the e-field is calculated<sup>3</sup>,

$$I = S = \frac{1}{2} E \times H = \frac{E^2}{2\eta}, \quad (2.33)$$

where  $S$  is the Poynting vector,  $I$  is intensity,  $E$  is the e-field,  $H$  is the magnetic field and  $\eta$  is the impedance in free space. Consequently, the time varying intensity detected is

$$I(t) = \frac{E_0^2}{2\eta} \left( \sum_{n=-\infty}^{\infty} J_n \left( \frac{\beta}{\omega_m} \right) \cos \left( \omega_L t + n(\omega_m t + \phi + \frac{\pi}{2}) \right) \right)^2. \quad (2.34)$$

This can be simplified by defining  $I_0 = \frac{E_0^2}{2\eta}$ ; however, the second part of the equation still consists of an infinite number of sinusoidal signals squared. Fortunately, since the magnitudes are controlled by Bessel functions, the number of sinusoidal signals is

essentially finite; however, experimentally, there are over  $10^5$  significant sidebands that interact. For discussion purposes, the number of sidebands is reduced in the following paragraphs.

Visualizing the source of the harmonic signals in the time domain is cumbersome; therefore, it is best to convert the laser e-field profile to the frequency domain, then graphically convolving the signals to illustrate the source of the harmonic intensity signals. The Fourier transform of the e-field results in delta functions spaced by the modulation frequency. Figure 2-1 illustrates the magnitude plot of laser frequency spectrum for a modulation index of 5. Figures 2-2 and 2-3 illustrate the phase plot for the positive and negative frequencies. Note the effect that the Bessel functions have on the phase angle, i.e., for odd values  $n$ ,  $J_n = -J_{-n}$ . This results in a  $180^\circ$  shift for odd sidebands left of the  $\omega_0$ . Also, the angle information for the negative frequency signal reflects that the even sidebands are actually sine functions, i.e., there is a  $180^\circ$  shift from their positive frequency counterparts.

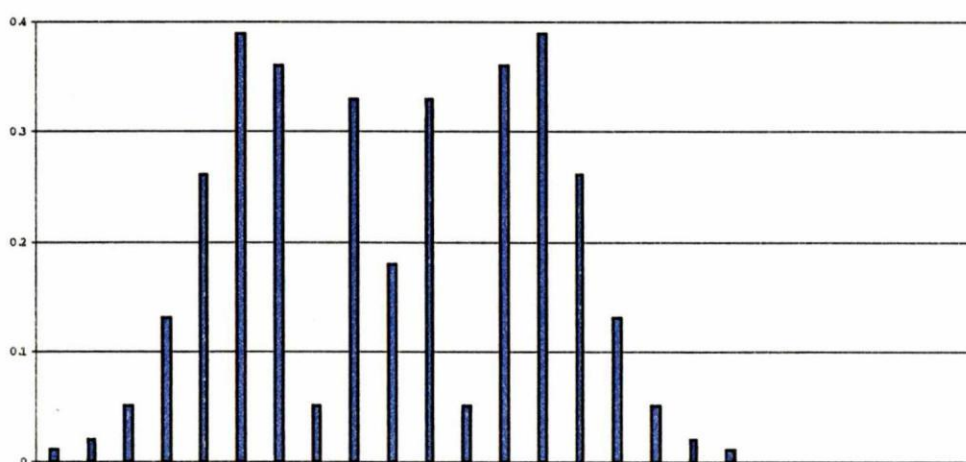
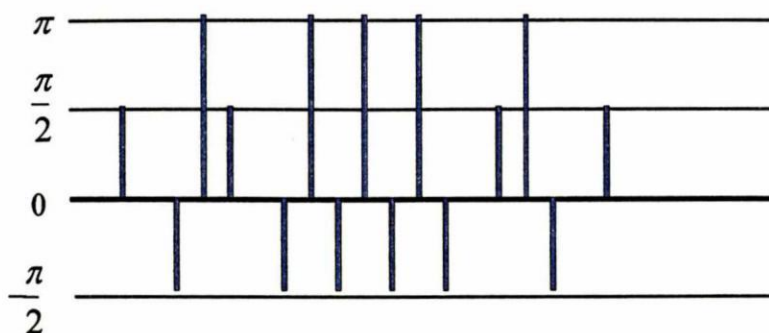
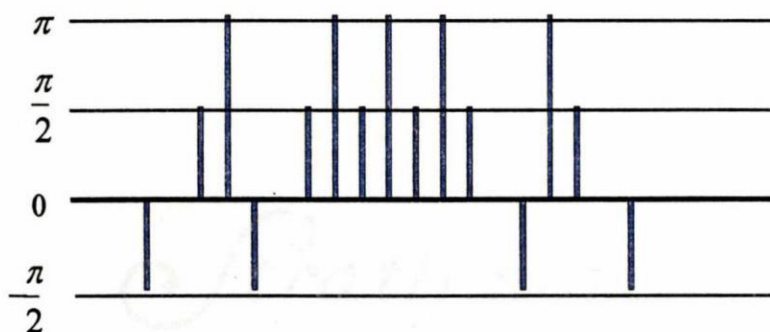


Fig. 2-1 Sideband magnitude plot of a modulation index of 5.



**Fig. 2-2 Angle information positive frequency sidebands.**



**Fig. 2-3 Angle information negative frequency sidebands.**

Figure 2-1 graphically shows the results of the convolution before shifting the signal. In the absence of absorption, the sum of the magnitude and phase information equals one, i.e., all of the intensity data is contained in the direct current signal. However, if an absorption feature were present, an imbalance in the sideband magnitudes would distribute some signal power through the harmonics. Absorption profiles will be discussed in greater detail in the next chapter; however, it is also important to understand the absence of the harmonic signals in pure wavelength modulation when an absorption feature is not present.

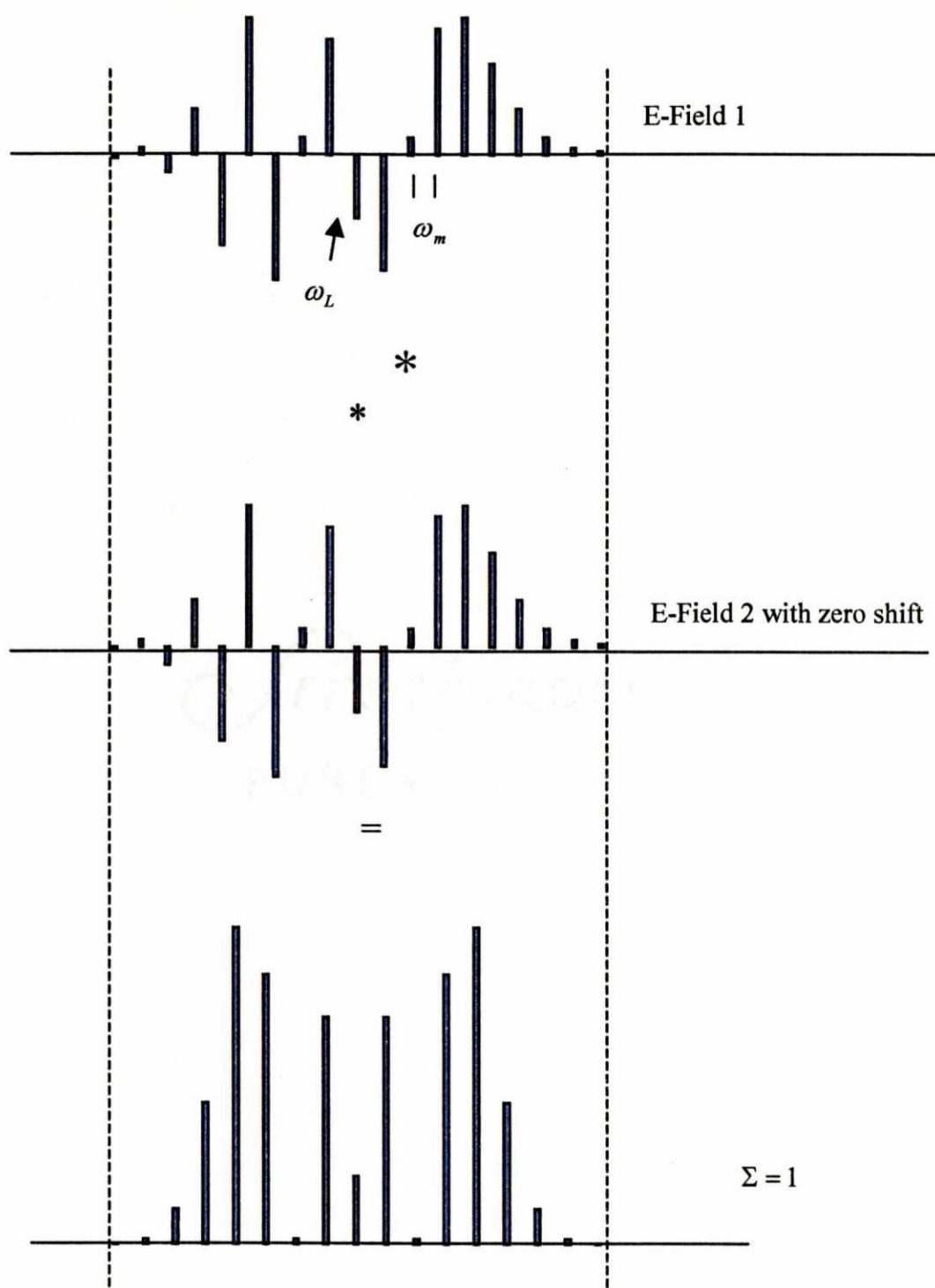


Fig. 2-4 DC signal generation with no absorption line.



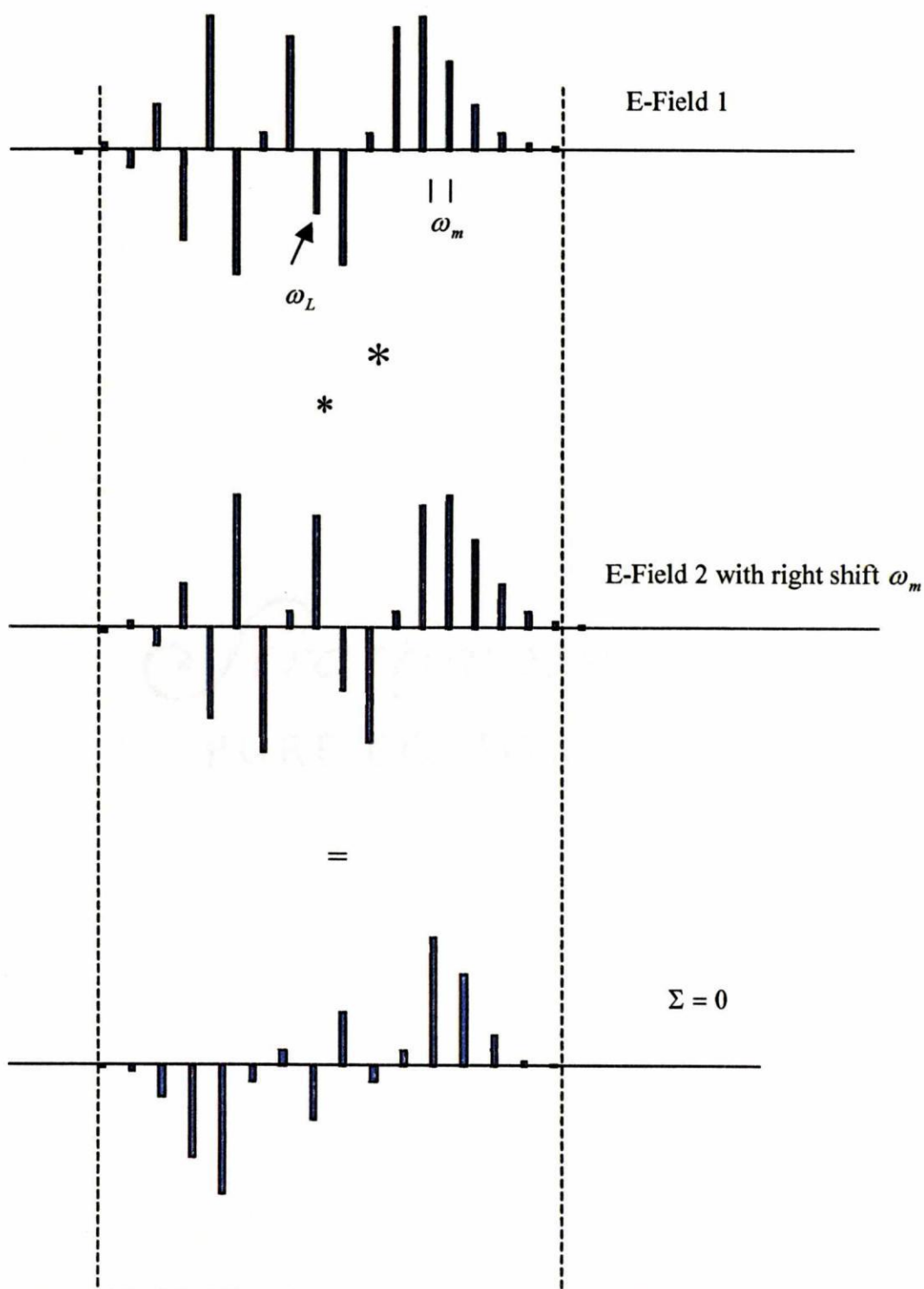


Fig. 2-5  $N_1$  equals zero in the absence of an absorption line.

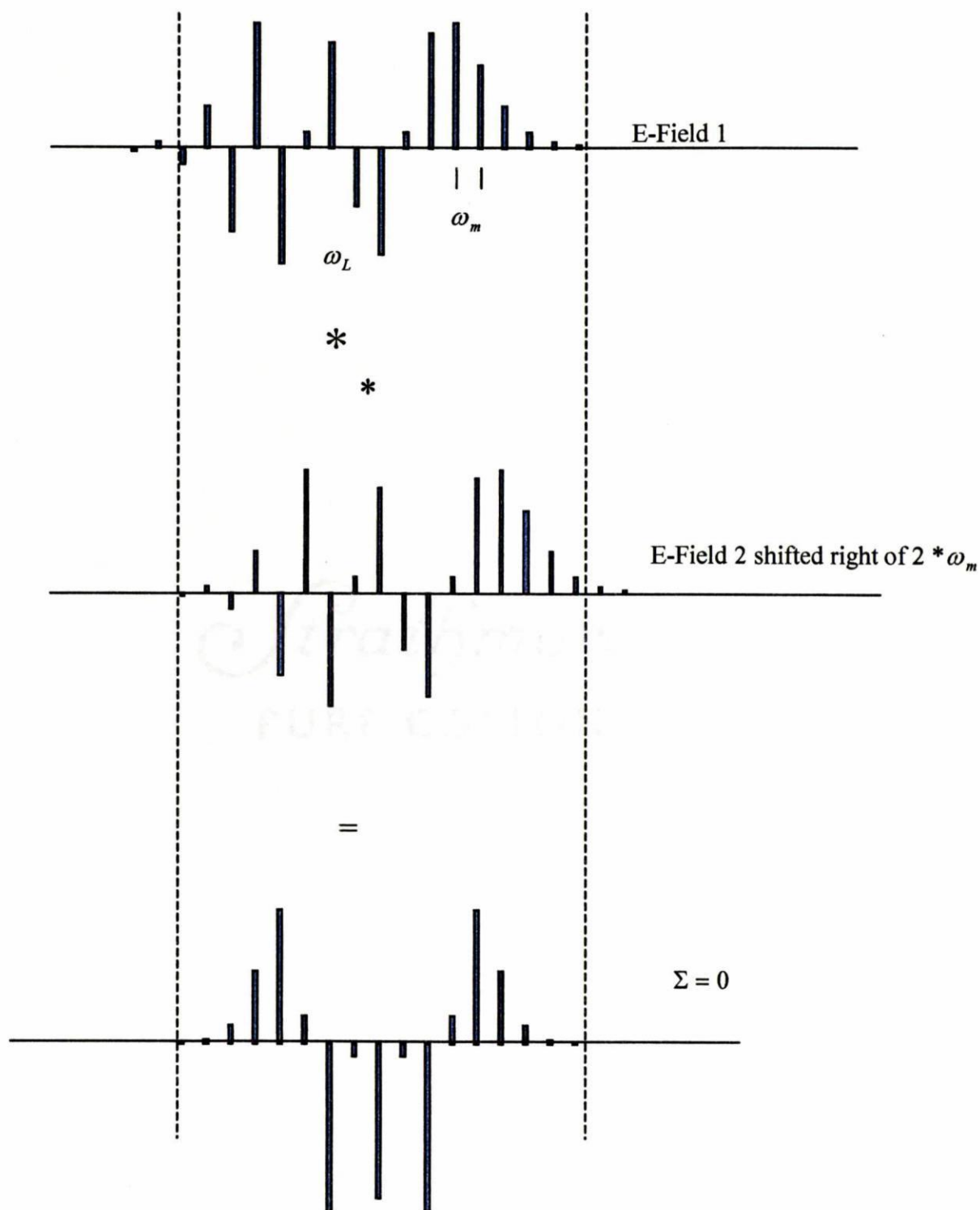


Fig. 2-6  $N_2$  equals zero in the absence of an absorption line.

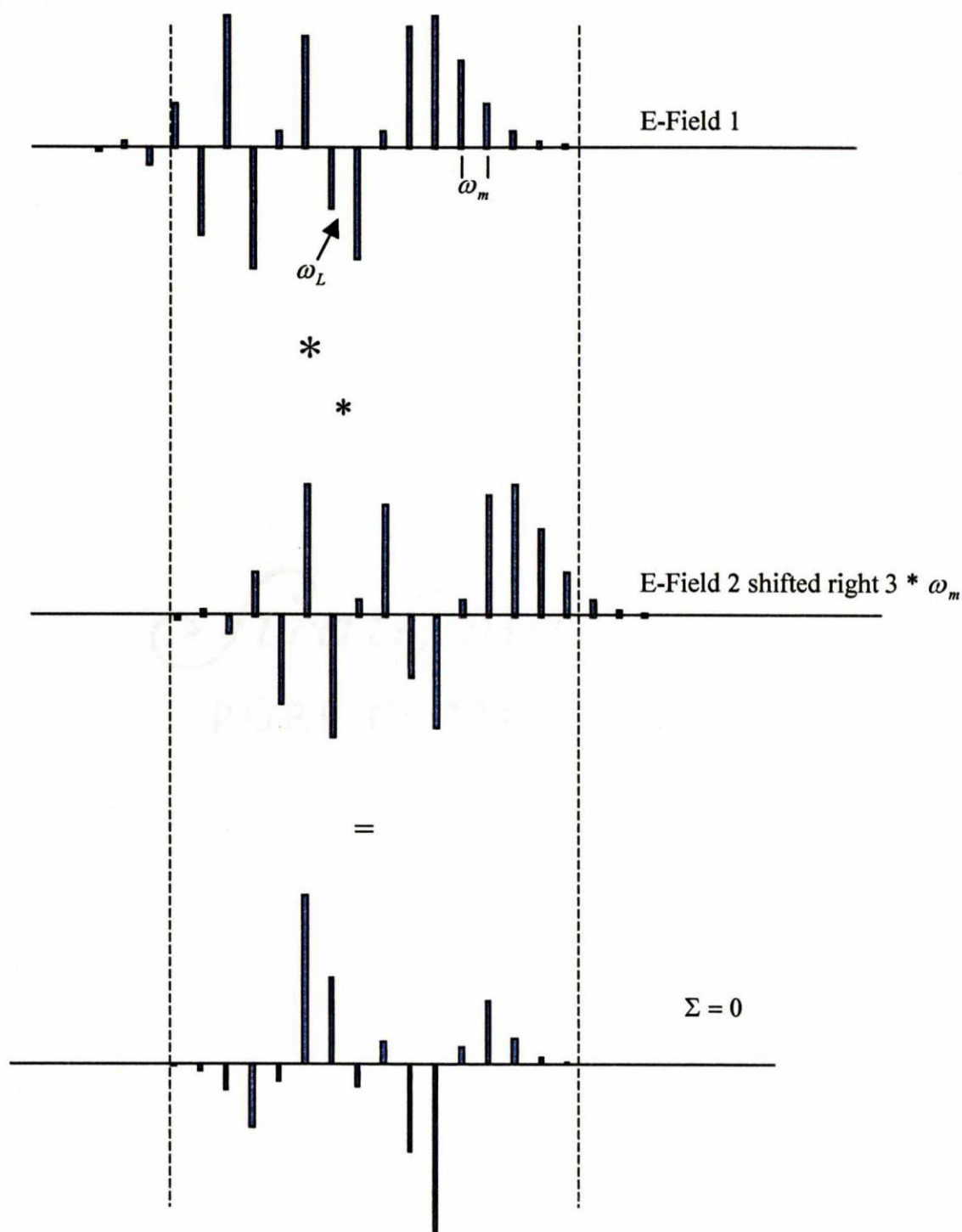
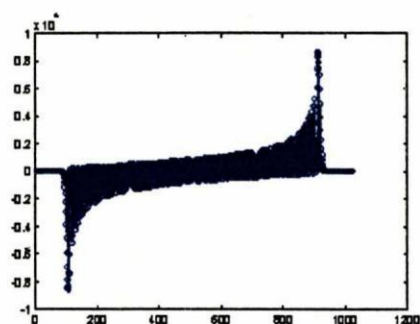


Fig. 2-7  $N_3$  equals zero in the absence of an absorption line.

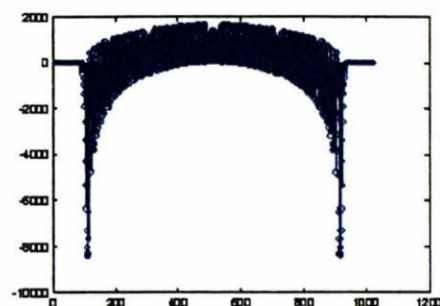
Therefore, figures 2-4 through 2-7 are presented to show how the first few harmonic signals would be developed. In figure 2-5, the convolution has continued by shifting the lower profile by the modulation frequency, i.e., the difference between the sidebands before the multiplication is  $\omega_m$ . It can be seen that the sum of the magnitudes; however, it is easy to imagine that an absorption feature that is not centered on the laser profile would cause an imbalance, i.e., the magnitude of some of the sidebands would be reduced by absorption and the sum would not be zero; therefore, a residual signal would be present. Figures 2-6 and 2-7 repeat the process for the second and third harmonics by shifting the laser profile before multiplying it.

The graphical convolution process (reverse an input, shift, multiply and then add) gives some unique insight into the generation of the harmonic signals. Each specific harmonic signal is developed by the multiplication between the laser profile and a reversed shifted version of itself where the harmonic is directly related to the amount of the shift. Therefore, the result after the multiplication can be used to show the effective probe signal. Figure 2-8 illustrates the effective laser probe signals for the first eight harmonics. The sources of several properties of wavelength modulation absorption profiles are evident in this figure. Note the symmetry of the probe signals of the odd harmonics. In the presence of a symmetric absorption profile centered on one of these profiles, the signal would still be balanced, i.e., the sum would still be zero. Therefore, as expected in a derivative-like signal, all odd harmonics are zero at line center. Also, imagining these profiles being swept past an absorption feature allows for the visual derivation of the qualitative signal.

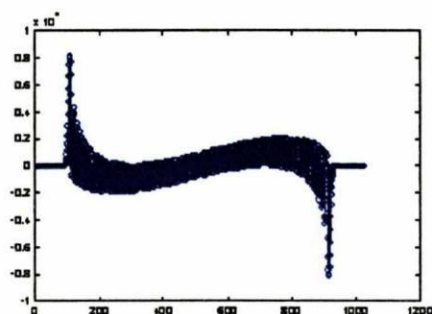




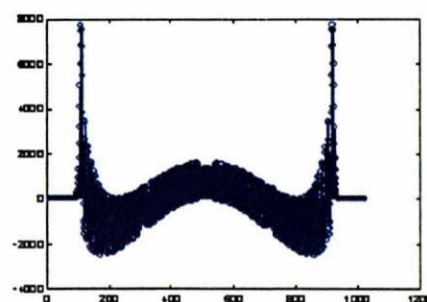
N1 Effective Laser Signal



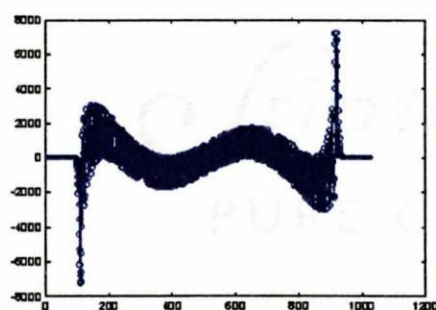
N2 Effective Laser Signal



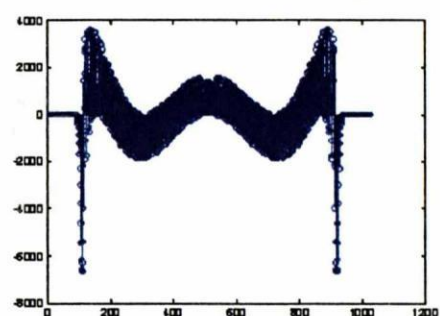
N3 Effective Laser Signal



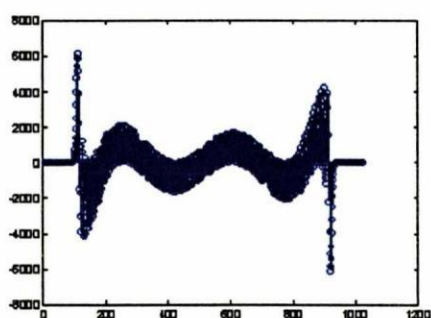
N4 Effective Laser Signal



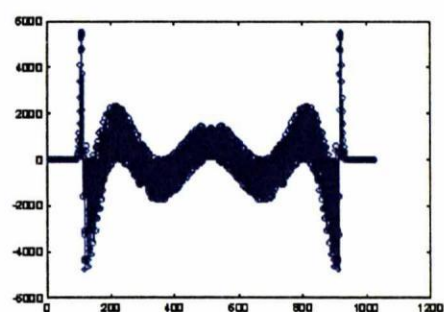
N5 Effective Laser Signal



N6 Effective Laser Signal



N7 Effective Laser Signal



N8 Effective Laser Signal

Fig. 2-8 Effective laser profiles for N1 though N8.

The previous paragraphs developed the frequency modulated laser profile; however, the intensity variations due to the modulated current have been neglected. In communications, amplitude modulation is mathematically defined as

$$E(t) = E_0 \left( 1 + \frac{r}{2} \sin(\omega_m t) \right) \cos(\omega_L t + \phi), \quad (2.35)$$

where  $r/2$  is the magnitude of the modulation. Squaring the e-field to determine the intensity results in the following

$$I(t) = I_0 \left( 1 + r \sin(\omega_m t) + \frac{r^2}{4} \sin^2(\omega_m t) \right) \cos^2(\omega_L t + \phi). \quad (2.36)$$

However, this does not match empirical data. Equation 2.36 implies that the magnitude of the N1 offset is directly related to the intensity, but experimentally it is independent. Therefore, the variation of intensity is not a result of conventional amplitude modulation, but rather a variation in the laser power, i.e., a modulation current is directly related to the electron hole pair generation. Intensity modulation is incorporated in the following equation:

$$I(t) = (I_0 + \cos(\omega_m t + \psi)) \left( \sum_{n=-\infty}^{\infty} J_n \left( \frac{\beta}{\omega_m} \right) \cos \left( \omega_L t + n(\omega_m t + \phi + \frac{\pi}{2}) \right) \right)^2, \quad (2.37)$$

where  $\psi$  is the phase difference between the modulation signal and the intensity modulation.

## CHAPTER III

### ABSORPTION PROFILES

As stated in the introduction, absorption profiles contain information about the temperature, pressure, and basic physics of a gaseous system. However, in order to extract that information, the source of the profiles has to be understood. This chapter derives the basic line shapes currently used for modeling experimental data.

#### 3.1 Doppler Profile

The intensity of light from a laser can be regarded as a stream of coherent photons. As light interacts with a medium, photons can be absorbed or stimulated as determined by the atomic or molecular composition of the medium and the energy or frequency of the photon,  $E = h\nu$ . If the photon energy matches the energy difference between two energy levels, whether it is electronic, vibrational, or rotational energy levels inherent to the molecule, then a transition can occur. In addition, for a transition to occur, the initial state must be populated. For example, for absorption, the lower state must be populated. When considering absorption, normally the transition is from a ground state, which is highly populated, to an excited state, which is normally open; therefore, in the following descriptions, the necessary population in the lower state is considered to be present.

For illustrative purposes, let us consider an electronic transition. The major features discussed below are, however, valid for all radiative transitions, spanning the

whole electromagnetic spectrum. Such a transition can be modeled quite adequately for most purposes, by the picture of an electron on a "spring" that leads to the Lorentz description. The fictitious spring in question is used to represent the quantum mechanical forces that arise when an electron feels an electric field that tends to displace it from a stationary state. As long as the imposed fields are smaller than any internal fields, the "restoring" force may be regarded as being proportional to the magnitude of the perturbation caused by the displacements. Hence, one often uses the simple harmonic oscillator model for a mass on a spring to describe the dynamics of an electronic transition induced by a photon. The frequency of the oscillation is controlled by the standard relationship,  $\omega_0 = \sqrt{K/m}$ . In this model, the oscillations are not damped; therefore, the oscillations are of infinite duration in the time domain and a delta function in the frequency domain.

One needs to clearly modify this simple model to account actual conditions one is likely to meet in any experiment. For example, in a gas, molecules are in motion. This motion results in a Doppler shift. Hence, when a molecule is moving away from an observer in the  $z$  axis, the frequency measured is  $\omega = \omega_0(1 - v_z/c)$ , where  $\omega$  is the detected radian frequency,  $\omega_0$  is the oscillation frequency,  $v_z$  is the molecular line-of-sight velocity, and  $c$  is the velocity of light. Therefore, the photon frequency required to interact with the oscillator depends on the molecule's velocity.

In an ideal gas, the distribution of the energy is considered to be Maxwellian<sup>7</sup>,

$$f(E) = Ae^{-\frac{E}{kT}}, \quad (3.1)$$



where  $k$  is Boltzmann's constant and  $T$  is the temperature. If the energy contained in a gas is considered to be strictly kinetic, i.e., the molecules are not interacting with any potential field, then energy can be equated to  $mv^2/2$ ,

$$f(v_z) = Ae^{\frac{mv_z^2}{2kT}}. \quad (3.2)$$

In order to solve for  $A$ , this equation has to be normalized to one. Since

$$\int_{-\infty}^{\infty} e^{-x^2} dx = \sqrt{\pi}, \quad (3.3)$$

setting  $x = \sqrt{m/2kT} v_z$ , then integrating

$$A \sqrt{\frac{2kT}{m}} \int_{-\infty}^{\infty} e^{\frac{mv_z^2}{2kT}} \sqrt{\frac{m}{2kT}} dv_z = 1, \quad (3.4)$$

results in  $A = \sqrt{m/2\pi kT}$ . Therefore, the standard Doppler velocity distribution is

$$W(v_z) = \sqrt{\frac{m}{2\pi kT}} e^{\frac{mv_z^2}{2kT}}. \quad (3.5)$$

As stated above, the frequency spectrum of an undamped oscillator is a delta function. Incorporating the Doppler shift from the motion, its spectrum is  $\delta(\omega - \omega_0(1 + v_z/c))$ . Therefore, in order to determine the frequency distribution of a medium containing numerous oscillators in motion, the spectrum of a molecule is multiplied with the velocity distribution and integrated over all velocities,

$$g(\omega) = \int_{-\infty}^{\infty} \delta\left(\omega - \omega_0 - \frac{\omega_0 v_z}{c}\right) \sqrt{\frac{m}{2\pi kT}} e^{\frac{mv_z^2}{2kT}} d\left(\frac{\omega_0 v_z}{c}\right) \frac{c}{\omega_0} = \sqrt{\frac{mc^2}{2\pi kT}} e^{\frac{mc^2(\omega - \omega_0)^2}{2kT\omega_0^2}}. \quad (3.6)$$

Thus, the Doppler line shape is a Gaussian profile<sup>5</sup>.

### 3.2 The Lorentzian Profile

The Doppler profile assumes that the lifetime of a transition is infinite, i.e., the oscillation is always present. Additionally, the Doppler profile neglects phase changing collisions, i.e., the wave train is continuous without interruption. In a gas at low pressure with few collisions, the Doppler profile is a good approximation of the absorption profile. However, as pressure and collisions increase, phase changing collisions have to be considered. The classical damped electron oscillator given by Siegman<sup>10</sup> provides an excellent model for a wave train with a finite period. Not only does this model give insight to absorption, it also models the phase shift associated with change of index of reflection. The foundation of this model is a simple damped harmonic oscillator,

$$\frac{d^2x}{dt^2} + \gamma \frac{dx}{dt} + \frac{K}{m}x = \frac{F}{m}, \quad (3.7)$$

where  $m$  is the mass of the electron,  $K$  is the spring constant,  $\gamma$  is the damping constant, and  $F$  is the force to initiate oscillations. As earlier, the electron and nucleus are modeled as a harmonic oscillator, but damping is added to show the finite period of the wave train due to phase changing collisions or the finite lifetime of the transition. If an electric field of a photon interacts with a molecule, it provides a force,  $-eE$ , to displace the electron, which in turn creates a dipole moment, given by  $-e^*x$ , where  $-e$  is the electron charge,  $E$  is the electric field and  $x$  is the distance of the displacement. In a medium containing numerous oscillators, the polarization density is equal to  $-N^*e^*x$ , where  $N$  equals the number of charges per unit volume. Substituting  $-eE$  for the force and multiplying both sides by  $Ne$  results in

$$Ne \frac{d^2x}{dt^2} + \gamma Ne \frac{dx}{dt} + Ne \frac{K}{m}x = \frac{d^2P}{dt^2} + \gamma \frac{dP}{dt} + \omega_0^2 P = -\frac{Ne^2E}{m}, \quad (3.8)$$

where  $P$  is the polarization density. Defining the time varying field and intensity as  $P = P \exp(j\omega t)$  and  $E = E \exp(j\omega t)$  results in the following

$$(-\omega^2 + \omega\gamma + \omega_0^2)P \exp(j\omega t) = -\frac{Ne^2 E \exp(j\omega t)}{m}. \quad (3.9)$$

Polarization can also be defined with a complex susceptibility,  $P = \epsilon_0 \chi E$ . Solving for

the susceptibility results in,  $\chi = \frac{P}{\epsilon_0 E}$ . Dividing the time variance from both sides of the

equation above and manipulating it to solve for susceptibility results in

$$\chi = \frac{P}{\epsilon_0 E} = -\frac{Ne^2}{m\epsilon_0} * \frac{1}{(-\omega^2 + j\omega\gamma + \omega_0^2)}. \quad (3.10)$$

Defining  $\chi_0 = -\frac{e^2 N}{m\omega_0^2 \epsilon_0}$  and the damping force  $\gamma$  as the width of the transition,  $\Delta\omega$

simplifies the above equation to

$$\chi = \chi_0 * \frac{\omega_0^2}{\omega_0^2 - \omega^2 + j\omega\Delta\omega}. \quad (3.11)$$

Since the primary concern is the line shape near resonance, the following approximations are made,

$$\omega_0^2 - \omega^2 = (\omega_0 + \omega)(\omega_0 - \omega) \approx 2\omega_0(\omega_0 - \omega), \quad (3.12)$$

and  $\omega = \omega_0$  in the second term in the denominator. Modeling electric susceptibility as complex number results in the following equation:

$$\chi = \chi' + j\chi'' = \chi_0 * \frac{\omega_0^2 (2\omega_0(\omega_0 - \omega))}{(2\omega_0(\omega_0 - \omega))^2 + (\omega_0 \Delta\omega)^2} - \chi_0 * \frac{j\omega_0^3 \Delta\omega}{(2\omega_0(\omega_0 - \omega))^2 + (\omega_0 \Delta\omega)^2} \quad (3.13)$$

Manipulating the equation results in

$$\chi' + j\chi'' = \chi_0 * \frac{\omega_0(\omega_0 - \omega)}{2} - \chi_0 * \frac{j\omega_0 \frac{\Delta\omega}{4}}{(\omega_0 - \omega)^2 + \left(\frac{\Delta\omega}{2}\right)^2} \quad (3.14)$$

The shape of the imaginary part is the Lorentzian, named after the pioneer of this model. The shape of the real part of electric susceptibility is approximately the derivative of the imaginary part with a slight asymmetry caused by the disappearance of the effect of  $\chi_0$  above the line shape. The effect of susceptibility on the propagation of light in medium can be seen by reviewing the electromagnetic propagation of a wave,  $Ee^{-jkr}$ . The wavevector contains the complex susceptibility,

$$k = \frac{\omega}{c} = \omega\sqrt{\epsilon\mu_0} = \omega\sqrt{\epsilon_0(1 + \chi' + j\chi'')}\mu_0 = \frac{\omega}{c_0}\sqrt{1 + \chi' + j\chi''},$$

$$k = k_0\sqrt{1 + \chi' + j\chi''}. \quad (3.15)$$

If  $\chi' \ll 1$  and  $\chi'' \ll 1$  then

$$k_0\sqrt{1 + \chi' + j\chi''} \approx k_0\left(1 + \frac{1}{2}(\chi' + j\chi'')\right). \quad (3.16)$$

This allows the separation of the wavevector into real and imaginary parts,

$$k = n - j\frac{\alpha}{2} = k_0\left(1 + \frac{\chi'}{2} + j\frac{\chi''}{2}\right), \quad (3.17)$$

where the index of refraction is  $n = 1 + \chi'/2$  and absorption coefficient is  $\alpha = k_0\chi''$ .

Therefore, the shape of the imaginary part of susceptibility is the absorption profile. Separating the Lorentzian profile from the imaginary part results in imaginary susceptibility of

$$\chi'' = -\chi_0 * \frac{\pi\omega_0}{2} g(\omega), \quad (3.18)$$



where the absorption line shape is

$$g(\omega) = \frac{1}{\pi} * \frac{\frac{\Delta\omega}{2}}{(\omega_0 - \omega)^2 + \left(\frac{\Delta\omega}{2}\right)^2}. \quad (3.19)$$

Therefore, the frequency spectrum of a single oscillator, which has a finite lifetime or suffers a dephasing collision, is a Lorentzian instead of the delta function used in the Doppler profile.

### 3.3 Voigt Profile

If the dephasing collisions and the Doppler effect are considered statistically independent, then the Lorentzian profile can simply replace the delta function in the Doppler equation before integrating over the velocity resulting in the Voigt line shape<sup>5</sup>,

$$g(\omega) = \left(\frac{m}{2\pi kT}\right)^{1/2} \int_{-\infty}^{\infty} \frac{1}{\pi} * \frac{\frac{\Delta\omega}{2}}{(\omega_0 - \omega - \Delta - \frac{\omega_0 v_z}{c})^2 + \left(\frac{\Delta\omega}{2}\right)^2} \times \exp\left(-\frac{mv_z^2}{2kT}\right) dv_z. \quad (3.20)$$

Notice that the factor  $\Delta$  is included to incorporate the change in frequency due to collisions, i.e., when molecules are close enough to each other, their energy levels are changed.

Modeling the Voigt is computationally expensive. Fortunately, the Voigt profile can also be modeled as the real part of the error function,  $w(z)$ .

$$\text{Re}[w(x', y)] = \frac{y}{\pi} \int_{-\infty}^{\infty} d\xi \frac{\exp(-\xi^2)}{y^2 + (x' - \xi)^2}, \quad (3.21)$$

where  $y$  is the dimensionless line width, effective frequency of broadening collisions divided by Doppler halfwidth,  $\Delta\omega_D/2$ ;  $x'$  is the separation from transition frequency, the  $(\omega - \omega_0 - \Delta)/(\Delta\omega_D/2)$ ;  $\xi$  is a dummy variable for integration. Improving the computational efficiency even more is Humilcek's approximation<sup>11</sup> of the error function.

### 3.4 Profile Narrowing

Although the Voigt incorporates the basics for the transition line shape in a gas, it lacks the elements to explain the small deviations detected in a precise measurement. For example, Rautian and Sobel'man<sup>12</sup> developed a line shape that incorporated a narrowing of the Voigt profile in a dense medium, Dicke<sup>13</sup> narrowing. As discussed in the derivation of the Voigt profile, collisions are not considered to have any affect on molecular velocity; therefore, the contribution of the Gaussian line shape to the Voigt is not altered by collisions. However, the inclusion of velocity-changing collisions, defined as collisions that change the velocity of the molecule but not the phase, can change the measurable velocity distribution.

Physically, it is hard to visualize the Doppler profile narrowing discussed by Rautian and Sobel'man. For example, their hard collision model considers that after every collision, the memory of the velocity prior to the collision is lost; its velocity is redistributed in the Maxwellian distribution. Therefore, the instantaneous velocity distribution of the molecules is always Maxwellian. If the energy of the gas in the medium remains the same, it is counter intuitive to expect a narrowing of Doppler profile due to velocity changing collisions. Varghese and Hanson<sup>14</sup> present an extreme case to

illustrate this phenomenon qualitatively. Consider a dense medium where a molecule is continuously involved in velocity changing collisions, i.e., the molecule conducts a random walk in velocity space. If the bulk gas is at rest, the mean velocity will approach zero even though the instantaneous velocity distribution is Maxwellian. Therefore, the value of measured velocity will depend on the time it takes to make the measurement. Spectrally, velocity in the line of sight results in a Doppler shift,  $\omega_0(1 + v_z/c)$ ; therefore, the velocity is measured over the period of a wave. In this extreme case, if there are enough collisions during one period of the fundamental frequency, i.e., if the path is much less than a wavelength,  $2\pi L \ll \lambda$ , where  $L$  equals the average velocity times the time between collisions, then the velocity measured will be the mean velocity of the molecule or in the case of a random walk, zero. However, in the other extreme, if collision were such that the path is much longer than the wavelength,  $2\pi L \gg \lambda$ , then velocity changing collision will just interrupt the wave train, broadening the Lorentzian part of the line width. Rautian and Sobel'man<sup>12</sup> derived the following equation to show this effect,

$$I(\omega) = \frac{1}{\pi} \operatorname{Re} \left\{ \frac{\int \frac{W(v) dv}{v + \frac{\Delta\omega}{2} - i(\omega_0 - \omega - \Delta - \frac{\omega_0 v}{c})}}{1 - \nu \int \frac{W_M(v) dv}{v + \frac{\Delta\omega}{2} - i(\omega_0 - \omega - \Delta - \frac{\omega_0 v}{c})}} \right\}, \quad (3.22)$$

where  $W(v)$  is the velocity distribution and  $\nu$  is the velocity changing collision frequency. The following changes were made to Rautian and Sobel'man's original equation for notation consistency: substituting  $\Delta\omega/2 = \Gamma$  and  $\omega_0/c = k$ , and  $\omega_0 - \omega$  was substituted back into the equation for  $\omega$ . Note, when the velocity distribution is



Maxwellian, the real part of the numerator is a Voigt profile with the Lorentzian width equal to  $\Delta\omega/2 + \nu$ . However, the denominator results in narrowing. If the velocity changing collision frequency is small, i.e., much less than the Doppler width, the second term denominator of the equation is negligible, and the line shape is a Voigt. However, in the other extreme, when the velocity changing collision frequency is much larger than the Doppler width,  $\nu \gg \Delta\omega_D$ , the second term in the denominator can approach one at line center, i.e., the second term of the denominator is simply an inverted Voigt weighted by the velocity changing collision frequency. When normalized, the center is larger than the Voigt's and narrowed on the sides; however, the wings are larger due to the inclusion of the velocity changing collision frequency in the Lorentzian portion of the Voigt.

Varghese and Hanson replaced these computational difficult integrations of the Voigt with the error function resulting in

$$NG(x', y, \zeta) = \text{Re} \left[ \frac{w(x', y + \zeta)}{1 - \sqrt{\pi} \zeta w(x', y + \zeta)} \right], \quad (3.23)$$

where  $\zeta$  is the dimensionless value of the velocity-changing collision frequency divided by the Doppler width. Note the change of variables in the error function from the definition used in the definition of the Voigt. The deviation from the unperturbed radiation frequency,  $x'$ , remains the same, but the velocity-changing collision frequency has been added to the collisional broadening frequency,  $y + \zeta$ .

Numerous other line shapes that are available<sup>15</sup> include speed dependent asymmetries and collision correlation effects. However, they are currently not used to model any experimental data. Therefore, they are excluded from this thesis. However, future precision may require the addition of these shapes.



## CHAPTER IV

### EXPERIMENTAL DATA

Previous chapters developed the theory of WMS and absorption line profiles. This chapter discusses experimental data; however, it is directed at some important features of the method, i.e., the ratioing of harmonic information, pressure vs. harmonic curves and modeling several absorption profiles on the same sweep.

#### 4.1 Ratioing Harmonic Information

As discussed in previous chapters, the harmonic information measured experimentally in WMS is simply the Fourier series coefficients of the intensity variations detected at the photodiode. Figure 4-1 shows the experimental setup. The intensity variations come from two sources, intensity modulation in the laser, and absorption. The intensity modulation from the laser is due to carrier modulation in the laser and manifests itself as an offset in the N1 signal and distortions in the lobes of the harmonic signals caused by absorption. The intensity variations from the absorption are due to the laser probing an absorption profile while the center frequency is modulated. The addition of a ramp sweeps the center frequency of the modulated laser across the frequency spectrum, probing different portions of the absorption profile resulting in changes in the Fourier coefficients. The resulting harmonic signals approach the derivative of the line shape as the modulation index approaches zero. Although this is a simple concept, exploiting it is difficult. The sinusoidal sampling of a nonlinear profile leads to complex intensity variations.

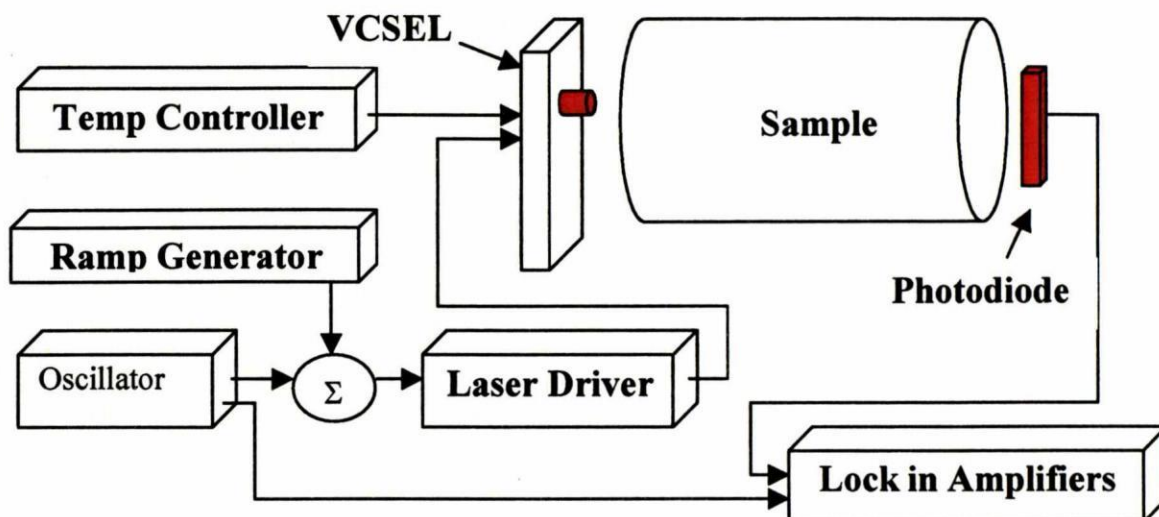


**Fig. 4-1 Experimental Setup.**

Therefore, numerical methods are required to calculate the coefficients. Typically in modeling, the intensity variation of one cycle of the modulation is divided into one thousand discrete points, which requires the calculation of the magnitude of the absorption at each of these points. This intensity variation is then multiplied by the sinusoid harmonic for the appropriate coefficient and the product is summed over the cycle. Finally, the center frequency of the modulation is stepped to the next frequency, simulating the ramp, and the calculation is repeated. The entire process for five thousand steps calculating eight harmonics requires approximately nine minutes on a 700 MHz PC for a simple profile. The model is imported into EXCEL and compared with experimental data. If the model does not match the experimental data, a profile parameter is adjusted to improve the match. This process is quite subjective and can be time consuming. However, by analyzing the ratio of the magnitudes of even harmonics at line center, the computation time can be reduced and the subjectivity of the measurement can be removed.

If the absorption is weak,  $|\alpha(\omega_{LC})L| \ll 1$ , then the Beer-Lambert law can be approximated as

$$I = I_0 e^{-\alpha(\omega)L} \cong I_0 * (1 - \alpha(\omega)L). \quad (4.1)$$

Therefore, the Fourier coefficients, neglecting amplitude modulation, can be approximated as

$$B_N = \frac{1}{T} \int_0^T [-I_0 * (\alpha(\omega_L - k_f A \sin(\omega_m t + \theta))L)] \sin(N(\omega_m t + \theta)) dt. \quad (4.2)$$

Tuning the center of the modulated laser to line center results in all odd harmonics being zero, with the exception of N1, which is offset by the intensity modulation, and even harmonics will be at their maximum with a reasonable modulation index. Evaluating the ratio of the magnitude of two even harmonics at line center results in

$$R_{N/K} = \frac{\int_0^T \alpha(\omega_L - k_f A \sin(\omega_m t + \theta)) * \sin(N(\omega_m t + \theta)) dt}{\int_0^T \alpha(\omega_L - k_f A \sin(\omega_m t + \theta)) * \sin(K(\omega_m t + \theta)) dt}, \quad (4.3)$$

where  $N$  and  $K$  are even harmonic numbers. Substituting the definition of the frequency dependent absorption coefficient,  $\alpha(\omega) = n\bar{\sigma}g(\omega)$ , into equation 4.3 and reducing it results in

$$R_{N/K} = \frac{\int_0^T g(\omega_L - k_f A \sin(\omega_m t + \theta)) * \sin(N(\omega_m t + \theta)) dt}{\int_0^T g(\omega_L - k_f A \sin(\omega_m t + \theta)) * \sin(K(\omega_m t + \theta)) dt}. \quad (4.4)$$

If the line shape is assumed, the only unknown in this equation is the line width. Therefore, the ratio of two even harmonics results in a direct measurement of line width if the absorption is small. Numerically, this reduces the number of points to be



calculated to one sweep. Additionally, once the line width is known, the integrated absorption cross section can now be varied to match the magnitude of the data.

As absorption increases, due to line strength or path length, the small signal approximation for the exponential is no longer valid resulting in the following equation,

$$R_{N/K} = \frac{\int_0^T e^{-\alpha(\omega_L - k_f A \sin(\omega_m t + \theta))L} \sin(N\omega_m t + \theta_{LIA}) dt}{\int_0^T e^{-\alpha(\omega_L - k_f A \sin(\omega_m t + \theta))L} \sin(K\omega_m t + \theta_{LIA}) dt} \quad (4.5)$$

In this case, the ratio is much more complex. As the strength of absorption increases, the line shape is distorted. Thus, in addition to the line width, the combination of path length and line strength contributes significantly to the ratio. A single ratio can lead to a family of line width/strength combinations. Therefore, the ratio method is most effective in the small signal domain. Additionally, this method requires simultaneous measurements of at least two even harmonics; otherwise, the ratio could be contaminated by intensity variations in the laser.

The above procedure was used to measure RQ (7,8) in the oxygen A band. First the line was measured at 154 cm to ensure the absorption was in the small signal domain. The ratio of N2 to N8 was used to calculate the width half maximum line width of 0.0505 cm<sup>-1</sup> and an integrated cross section of 8.73E-24 cm/mol. The current accepted values from HITRAN<sup>16</sup> are 0.0558 cm<sup>-1</sup> and 8.83E-24 cm/mol in air. These profiles are presented in Figure 4-2. Additionally, the direct absorption profile is shown. The path length was then increased to 3219 cm, and 5279 cm, respectively, to move the signal out of the small signal approximation. The signals were then modeled using the parameters calculated at 154 cm and are presented in figures 4-3 and 4-4.



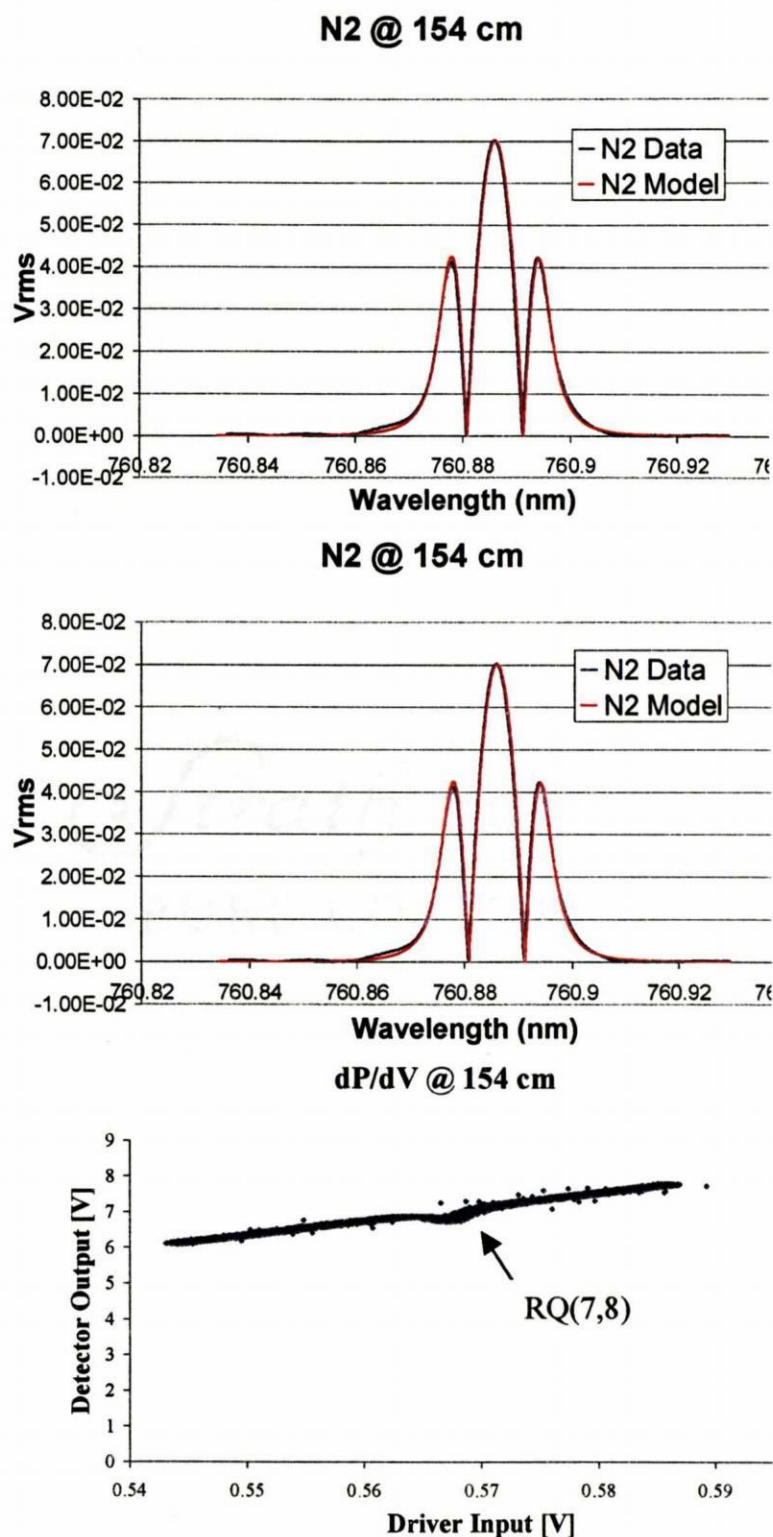


**Fig. 4-2** N2 and N8 harmonic signals of RQ (7,8) measured at 154 cm. Calculated models are shown in red and data shown in blue. Calculated line width is  $.0505 \text{ cm}^{-1}$  and line strength is  $8.78 \text{ cm/mol}$ .

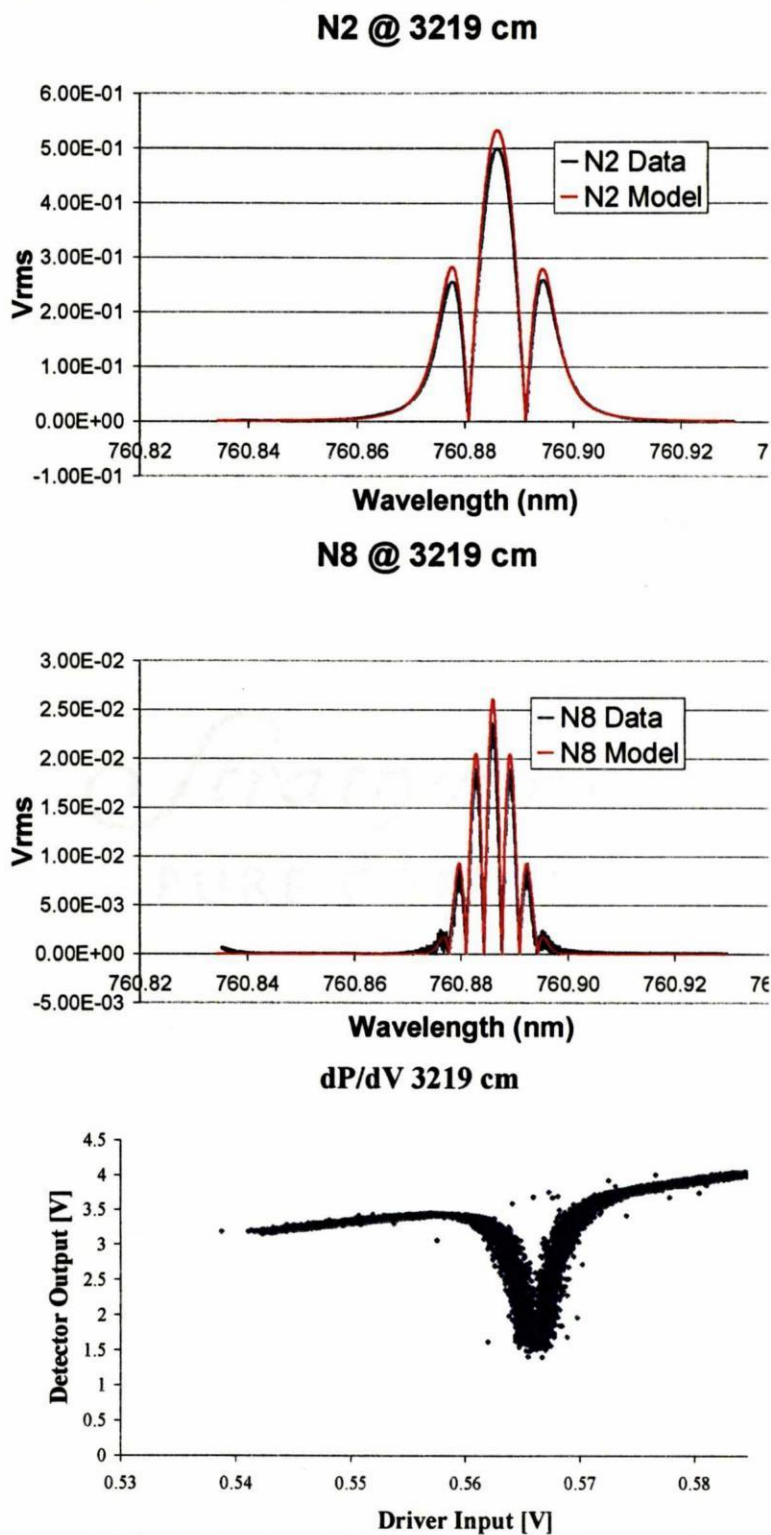


**Fig. 4-3 N2 and N8 harmonic signals of RQ (7,8) measured at 3219 cm. Calculated models are shown in red and data shown in blue. Calculated line width is  $.0505 \text{ cm}^{-1}$  and line strength is  $8.78 \text{ cm/mol}$ .**

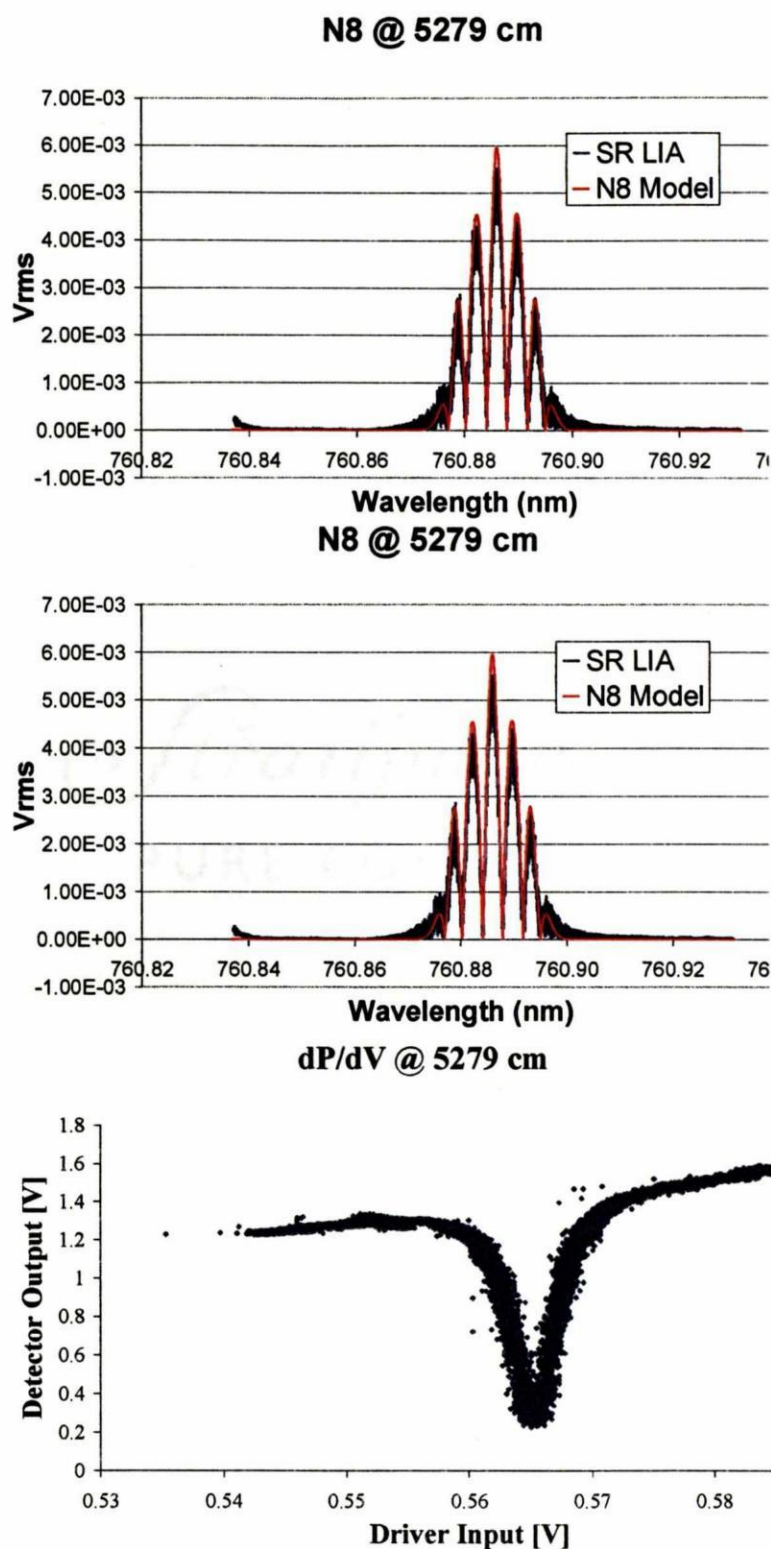


**Fig. 4-4 N2 and N8 harmonic signals of RQ (7,8) measured at 5279 cm. Calculated models are shown in red and data shown in blue. Calculated line width is  $.0505 \text{ cm}^{-1}$  and line strength is  $8.78 \text{ cm/mol}$ .**

the ratio matches. In addition, the model signal magnitudes at 5279 cm are also slightly larger than the data. Although these figures may not appear as good as previous data, they are completely void of normalizations. If normalized at each harmonic as done previously, these matches would be almost perfect.

## 4.2 Pressure vs. Harmonic Curves

Another well-documented phenomenon is the variation harmonic magnitudes with a change in pressure, (see figure 4-5). Physically, this is simply due to the change of the absorption profile due to collisions. There are two factors affecting the turning points of the harmonic magnitudes. First, the number of molecules increases the magnitude of absorption resulting in larger intensity variation at the detector; thus, a larger ac voltage is sent to the lock in amplifier. This accounts for the sharp increase at low pressures. Secondly, the increased number of molecules results in more collisions, increasing the line width. This changes the effective spectroscopy modulation index, i.e., line width divided by modulation width,  $HWHM / Ak_f = FWHM / \Delta\omega$ . (Note this modulation index definition is different from the standard communication modulation index used earlier. Due to a large difference in modulation frequency and absorption line width, the use of the standard modulation index definition would result in modulation indexes of over 100,000. The spectroscopic definition reduces this number and makes it more meaningful; however, it is a relative parameter.) This change in line width due to collisions is critical due to the nature of the sampling. This can easily be visualized by reviewing figure 1-4. The broadening of the sampled signal will result in a change in the



Fourier coefficients depending on how well it matches the harmonic of interest. The turning points also depend on the line shape. For example, Ried and Labrie<sup>17</sup> calculated that the optimum modulation index for N<sub>2</sub> signals for the Gaussian and Lorentzian line shapes was 2.2, which has been reproduced in MATLAB.

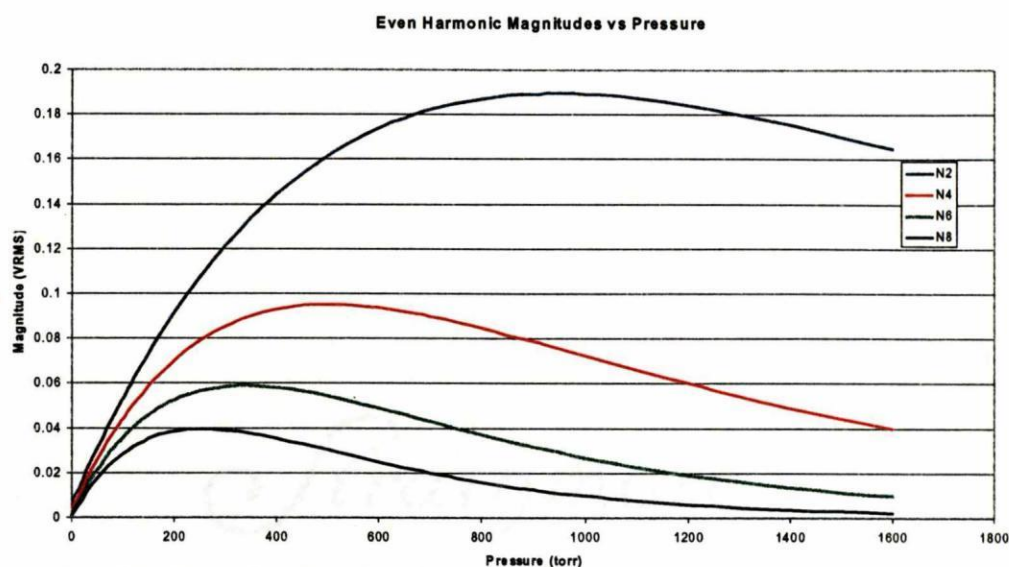


**Fig. 4-5 Theoretical Even Harmonic Magnitudes vs. Pressure for a Gaussian Line shape.**

An experiment was conducted in a chamber to measure this phenomenon using the RQ(7,8) oxygen line. Ratios were once again used to calculate line width; however, simultaneous measurements were not. The evolution of the direct absorption line profile is shown in figure 4-6. The broadening of the line is due to the increased collisions while the depth of the profile is caused by the increase in absorbers.

After modulation was added at one thousand hertz, the harmonic signals were recorded using a Lock-in-amplifier. The ratio resulted in a calculated line width of  $0.0487 \text{ cm}^{-1}$  and a line strength of  $8.13\text{E-}24 \text{ cm/mol}$ . HITRAN<sup>16</sup> indicates a line width of 0.0508 in oxygen. Figures 4-7, 4-8, 4-9, and 4-10 show the experimental versus model magnitudes for N<sub>2</sub>, N<sub>4</sub>, N<sub>6</sub> and N<sub>8</sub>, respectively. Note that although the model and data match qualitatively, lower harmonics have a mismatch in magnitude.

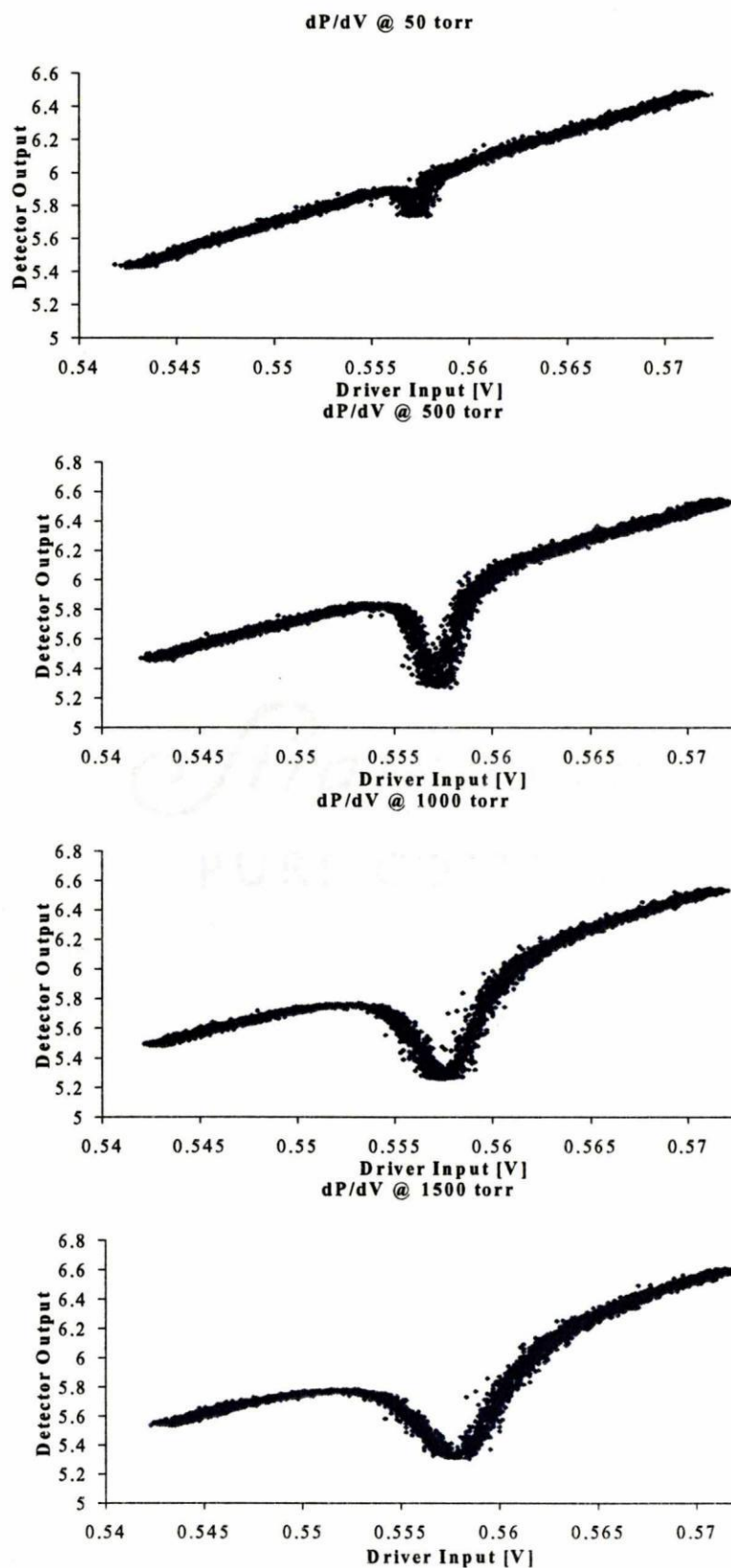


**Fig. 4-6 Direct absorption of RQ(7,8) at 50, 500, 1000, and 1500 torr.**

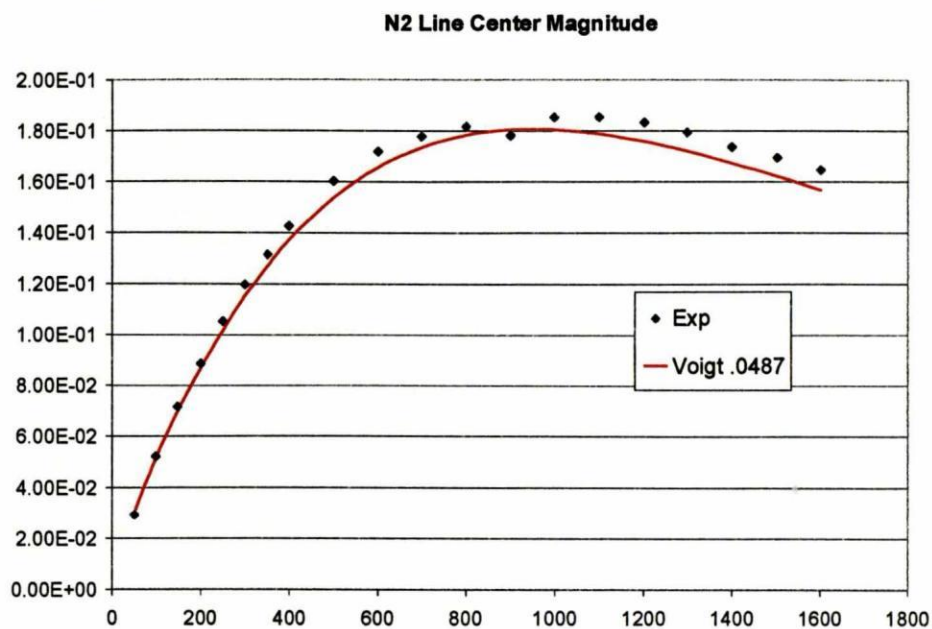


**Fig. 4-7 N2 Line center Magnitude vs. pressure for RQ(7,8) in oxygen. Modeled as a Voigt with a line width of  $0.0487 \text{ cm}^{-1}$ .**

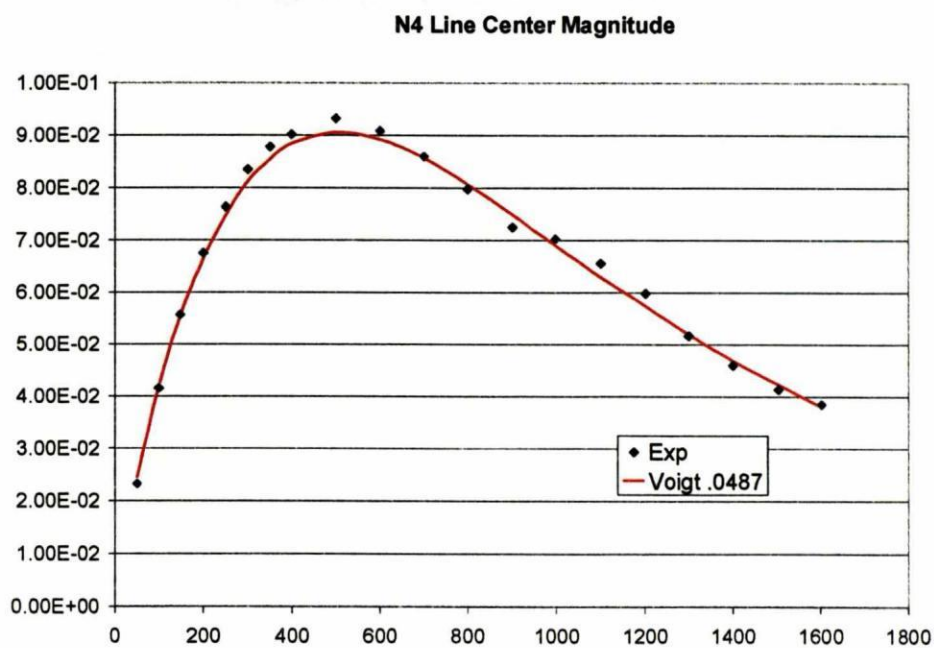


**Fig. 4-8 N4 Line center Magnitude vs. pressure for RQ(7,8) in oxygen. Modeled as a Voigt with a line width of  $0.0487 \text{ cm}^{-1}$ .**

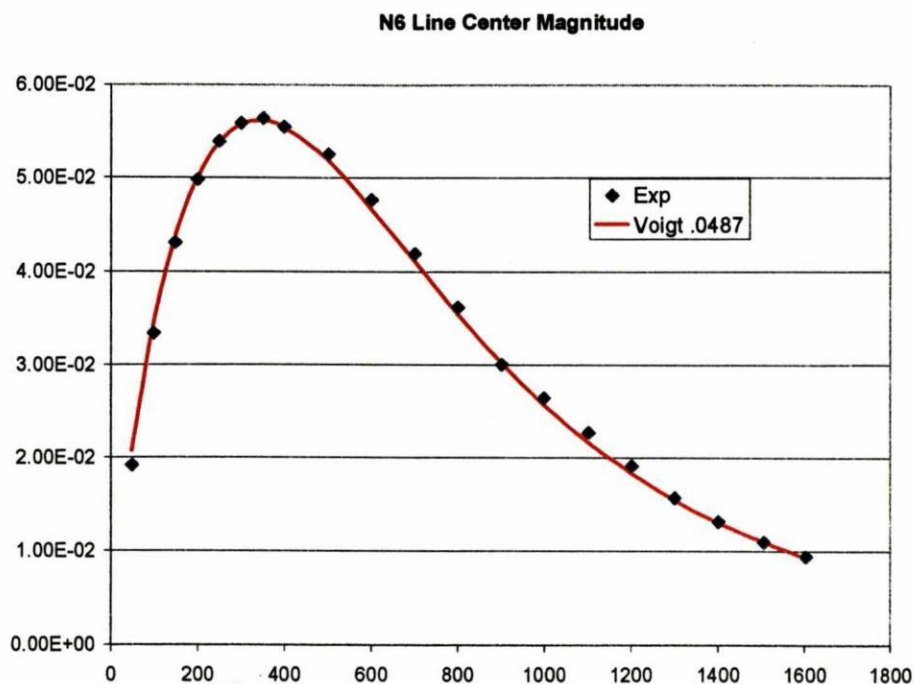


**Fig. 4-9 N6 Line center Magnitude vs. pressure for RQ(7,8) in oxygen. Modeled as a Voigt with a line width of  $0.0487 \text{ cm}^{-1}$ .**

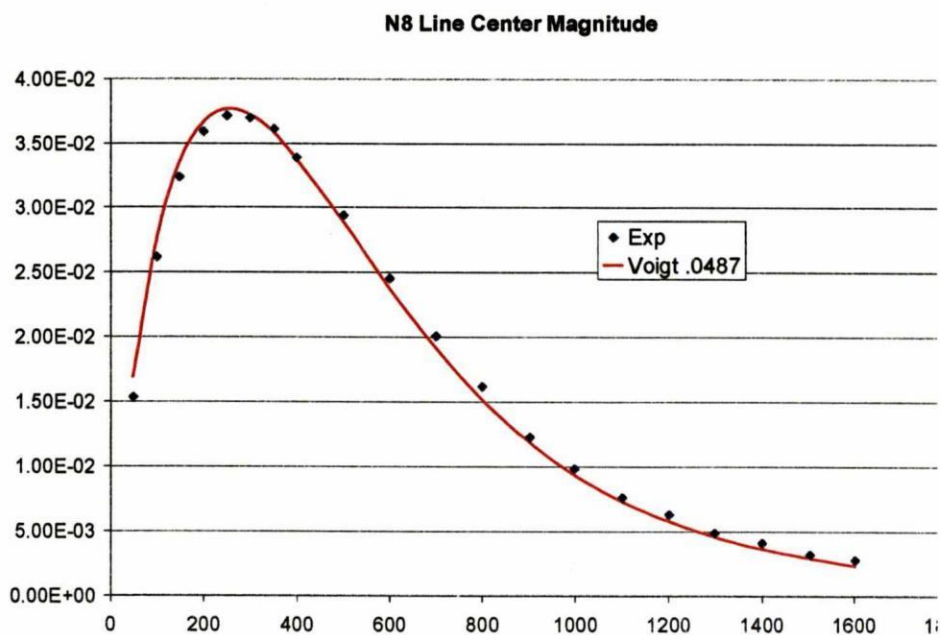


**Fig. 4-10 N8 Line center Magnitude vs. pressure for RQ(7,8) in oxygen. Modeled as a Voigt with a line width of  $0.0487 \text{ cm}^{-1}$ .**



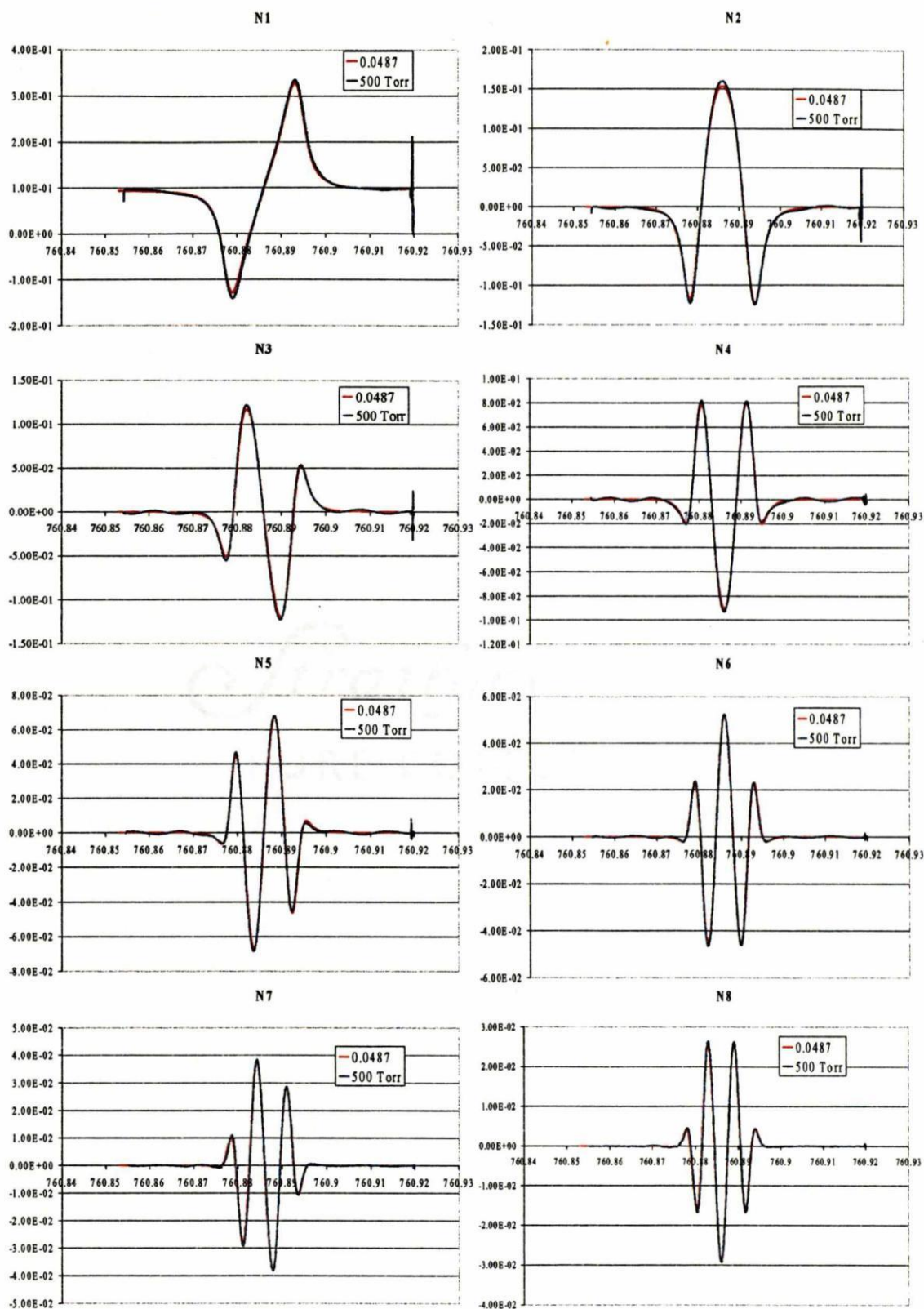


Fig. 4-11 Profiles for N1 through N8 for RQ(7,8) at 500 torr

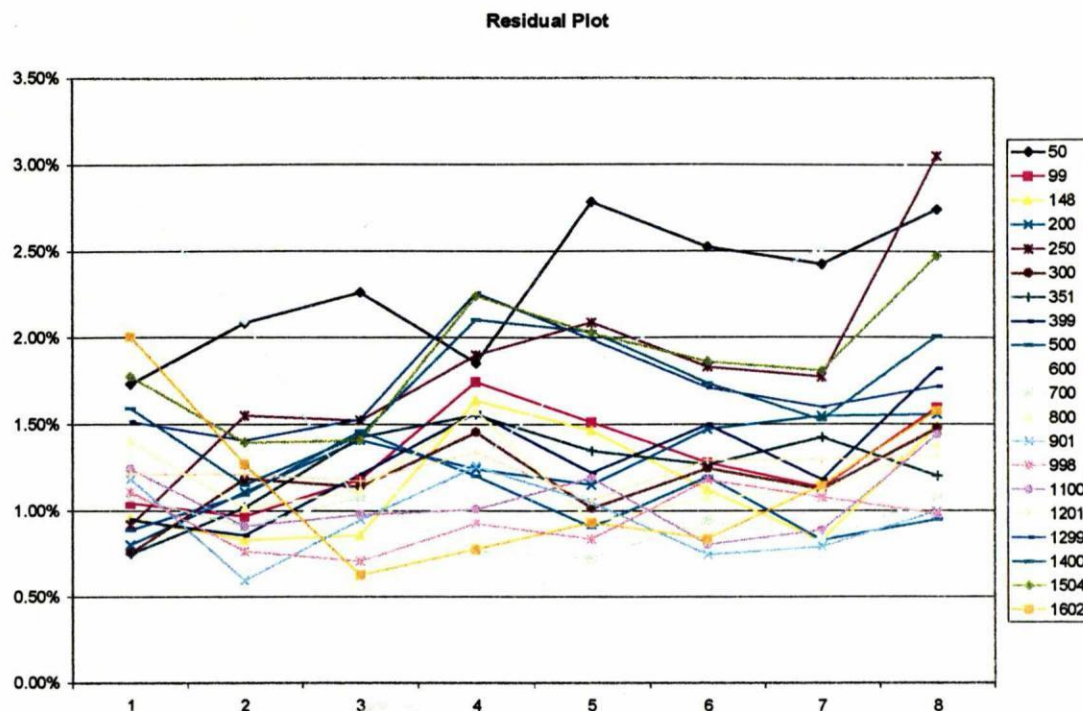


Fig. 4-12 Residue vs. Harmonic order for the comparison of a Voigt model of RQ(7,8) with a line width of  $0.0487 \text{ cm}^{-1}$  and line strength of  $8.13 \text{ cm/mol}$  from 50 torr to 1602 torr.

The frequency spectra for 500 torr are shown in Figure 4-11. Although the magnitudes for the model are lower than the experimental data at line center, the match across the spectrum is excellent. Figure 4-12 shows the RMS error for all pressures and harmonics.

This experiment is very similar to the experiment conducted by Bullock<sup>18</sup>. Note, however, that for the experiment described in this thesis a Voigt line shape was used as the model instead of the Rautian Sobel'man with analogous results, i.e., similar residues. Unfortunately, there were two errors in the computer model of the Rautian Sobel'man. First, the narrowing parameter was not included in the line width portion of the complex error function (See equation 3.23 above). Secondly, this Varghese and Hanson approximation is inherently not normalized, i.e., the numerator integrates to an area of

$\sqrt{\pi}$  ; however, if the narrowing parameter is not equal to zero, the denominator will always increase this area. This would need to be corrected numerically.

### 4.3 Modeling several lines with a single ramp

Although it seems a simple extension of WMS, increasing the length of the ramp to include several lines for modeling results in several problems. First, any nonlinearity in the ramp causes errors in the frequency of the line center. Secondly, inaccurate modeling of the intensity modulation results in errors in the qualitative shape and magnitude of the harmonics. Previously, these problems were overcome by numerous normalizations, i.e., normalizations at each harmonic for each line. However, the information contained in the ratio of the harmonics is lost. Therefore, it is important to model the data without any normalizations to mine all of the information.

An experiment was conducted to include four lines in one sweep; RR(13,13), RR(13,13)\*, RR(43,43), and RQ(12,13). Table 4.1 presents the calculated data versus the HITRAN data for these lines.

Line	HITRAN		Calculated	
	HWHM [cm <sup>-1</sup> ]	$\sigma$ [cm/mol]	HWHM [cm <sup>-1</sup> ]	$\sigma$ [cm/mol]
RR(13,13)	0.0519	5.67E-24	0.0455	4.75E-24
RR(13,13)*	0.0519	1.15E-26	0.0455	9.62E-27
RR(43,43)	0.0398	1.32E-28	0.0336	1.1035E-27
RQ(12,13)	0.0519	1.41E-26	0.0455	1.177E-26

Table 4-1 Comparison of experimental calculations and HITRAN data.

Symbol \* indicates <sup>16</sup>O <sup>18</sup>O isotope.



Figure 4-13 shows the direct absorption of this sweep. Notice that only the strongest line, RR(13,13) is visible. Figures 4-14 through 4-16 show the power of WMS. Notice that the weaker lines are more visible at higher harmonics. Although this experiment has been conducted before, these models used here are not normalized. The laser was characterized, i.e., the intensity output for a given input was measured and the magnitude of the harmonics was simply controlled by the amount of absorption.

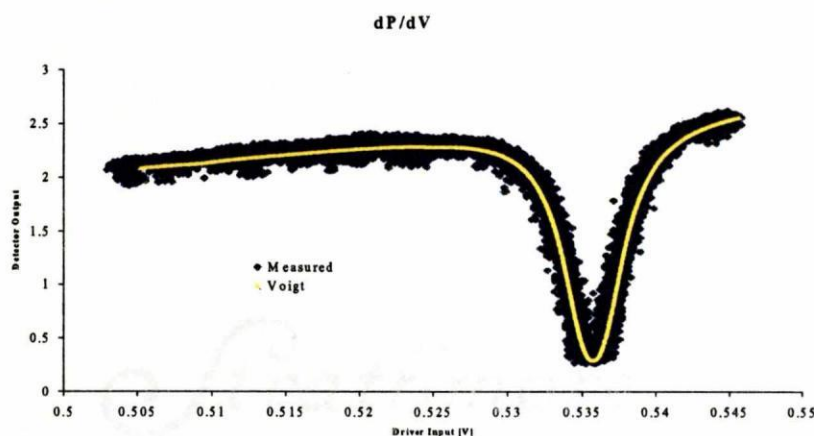


Fig. 4-13 Direct absorption of RR(13,13), RR(13,13)\*, RR(43,43), and RQ(12,13).

Symbol \* indicates  $^{16}\text{O } ^{18}\text{O}$  isotope.

### Second Harmonic (N=2) Detection

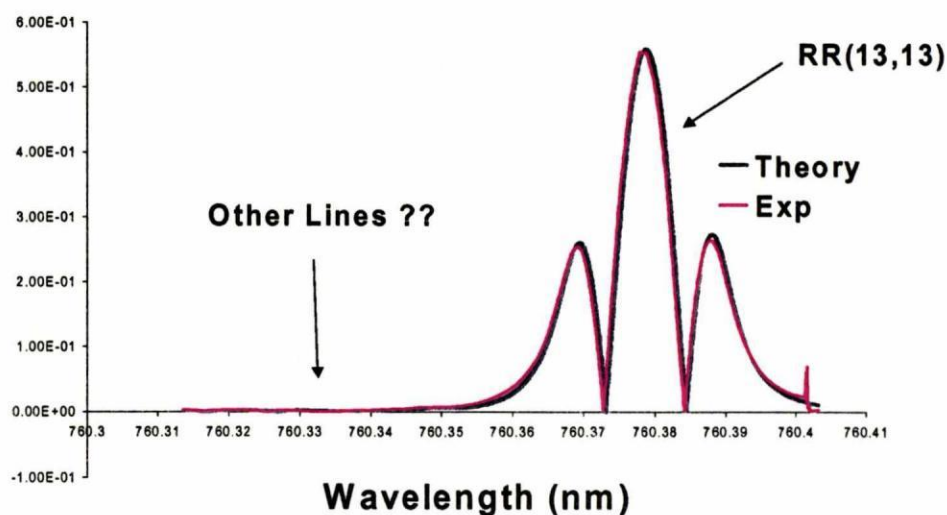


Fig. 4-14 N2 profile for RR(13,13), RR(13,13)\*, RR(43,43), and RQ(12,13).

Symbol \* indicates  $^{16}\text{O } ^{18}\text{O}$  isotope.



### Seventh Harmonic (N=7) Detection

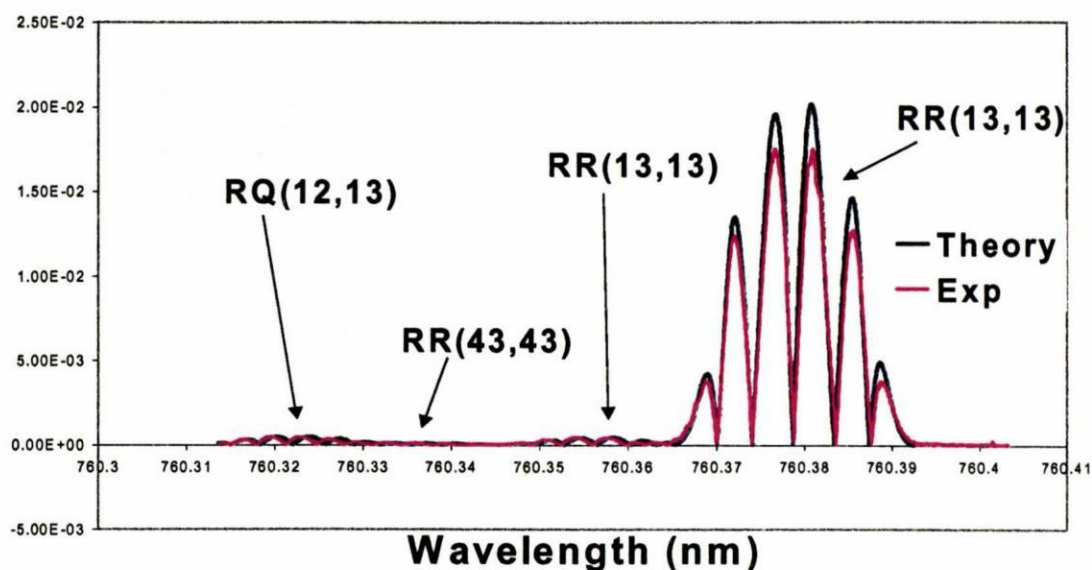


Fig. 4-15 N7 profile for RR(13,13), RR(13,13)\*, RR(43,43), and RQ(12,13).

Symbol \* indicates  $^{16}\text{O}$   $^{18}\text{O}$  isotope.

### Eighth Harmonic (N=8) Detection

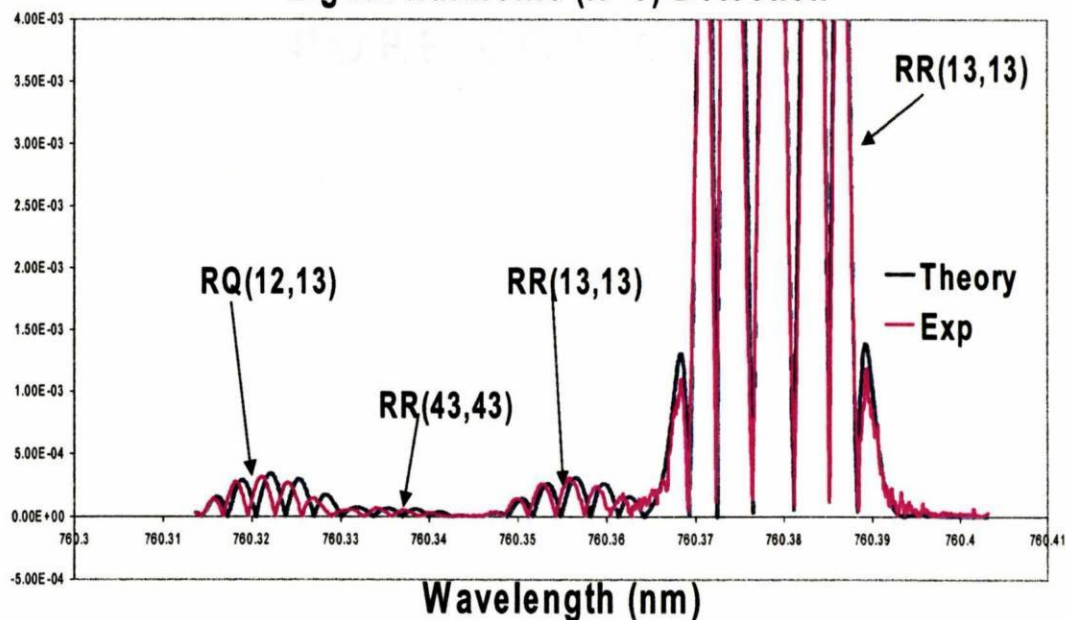


Fig. 4-16 N8 profile for RR(13,13), RR(13,13)\*, RR(43,43), and RQ(12,13).

Symbol \* indicates  $^{16}\text{O}$   $^{18}\text{O}$  isotope.

Notice on figure 4-16 that a small non-linearity in the ramp is visible, i.e., the relative position of the lines is slightly offset.

## CHAPTER V

### FUTURE WORK

Currently, the precision of the experiments performed in this research is good. As shown in figure 4-11, the residual between the model and experimental data is less than 3.00% for numerous pressures and harmonics. However, there are several ways to improve the precision. For example, taking simultaneous measurements of multiple harmonics to alleviate intensity variations for ratioing. We are just starting to do this on a regular basis. Also, automating the measurement and modeling will improve precision. Ratioing removes the subjectivity, which allows for automation. This will allow for results at almost real time, which will also reduce errors due to any drifts in the laser characteristics.

In addition, in all the measurements discussed previously, the line shape was known *a priori*. Therefore, by ensuring the absorption profile was in weak absorption environment by controlling the path length, the line shape parameters were solved by varying them independently. However, more complex line shapes do not allow for this independent variation. For example, the narrowed Voigt, or Rautian Sobel'man profile, contains two parameters that control the conventional line width, the narrowing parameter and the collision line width. The easiest method of separating the affects of these two parameters is to vary the pressure. This inherently removes some absorption lines from the weak absorption approximation due to their line strength and density. Therefore, a non-linear least-squares fit between the actual and experimental data is required to validate the parameters. The least-squares errors were painstakingly calculated using EXCEL. The automation of the calculations using MATLAB will

greatly enhance these measurements. Additionally, the ability to obtain precise automated measurements of line shapes will allow for the mining of the information contained within them on a real time basis.

The only approximation currently involved in the models is the exclusion of the laser line widths. The laser is approximated by a delta function, which is currently justified by the ratio of absorption profile line width to laser line width, approximately 50:1. In chapter II, a method for inclusion of laser line width was included; however, it has not been fully implemented. Although the computational cost of adding the line width is considered prohibitive, as precision increases it may be required for final measurements.

Finally, work is being conducted on determining the amount of entropy contained in each harmonic using communication theory. By quantifying the information in each harmonic, parameters, such as modulation index, can be selected prior to an experiment to enhance measurements. For example, certain features such as narrowing may be more pronounced at certain modulation indexes and harmonics. Entropy can be used to identify which harmonic will contain the most information on the feature being investigated allowing the investigator to focus their efforts.

WMS provides a cost effective means of obtaining information of a gaseous system through precise measurements of the transition line shape parameters. Although current experiments are providing good results, future work should result in a viable real time measurement device.



## REFERENCES

- [1] A.N. Dharamsi and Y. Lu, *J. Appl. Phys B*, **62**, 273 (1996).
- [2] A.N. Dharamsi and A.M. Bullock, *J. Appl. Phys B*, **63**, 283 (1996).
- [3] "Fundamentals of Photonics," B.A. Saleh, M.C. Teich, John Wiley and Sons, New York (1991).
- [4] G.V.H. Wilson, *J. Appl. Phys.*, **34**, 3276 (1963).
- [5] "Laser Electronics," J.T. Verdeyen, Prentice Hall, New Jersey (1995).
- [6] Y. Lu, Thesis, Old Dominion University, (1995).
- [7] G.C. Bjorklund and M.D. Levenson, *J. Appl. Phys B*, **32**, 145 (1983).
- [8] A. Jackson, Thesis, Old Dominion University, (1996).
- [9] "Modulation Theory," H.S. Black, D. Van Nostrand Co., Canada (1953).
- [10] "Lasers," A.E. Siegman, University Science Books, Mill Valley (1986).
- [11] J. Humelicek, *J. Quant. Spectrosc. Transfer*, **21**, 309 (1978).
- [12] S.G. Rautian and I.I. Sobel'man, *Soviet Phys*, **9**, 701 (1967).
- [13] R.H. Dicke, *Phys. Rev.*, **89**, 472 (1953).
- [14] P.L. Varghese and R.K. Hanson, *Applied Opt*, **23**, 2376 (1984).
- [15] R. Cisylo, *Phys. Rev. A*, **58**, 1029 (1998).
- [16] HITRAN'96 Molecular Database, L.S. Rothman, et al. (1996).
- [17] J. Ried and D. Labrie, *J. Appl. Phys B*, **26**, 203 (1981).
- [18] A.M. Bullock, Dissertation, Old Dominion University, (2000).



## APPENDIX

### MATLAB SIMULATION

The following program was written in MATLAB to demonstrate Wavelength Modulation in the Frequency Domain. The program provides a GUI with eight panels, displaying the absorption and laser profiles and the detected signals. Although this program is too slow to efficiently model experimental data, it provided tremendous insight to the theory and method. On the right, there are several edit boxes, which allow the entry of the center frequency,  $\Delta\omega$ , modulation frequency, sampling frequency and line width. Additionally, there is a menu to allow sweeping of the center frequency of the laser or the modulation index.

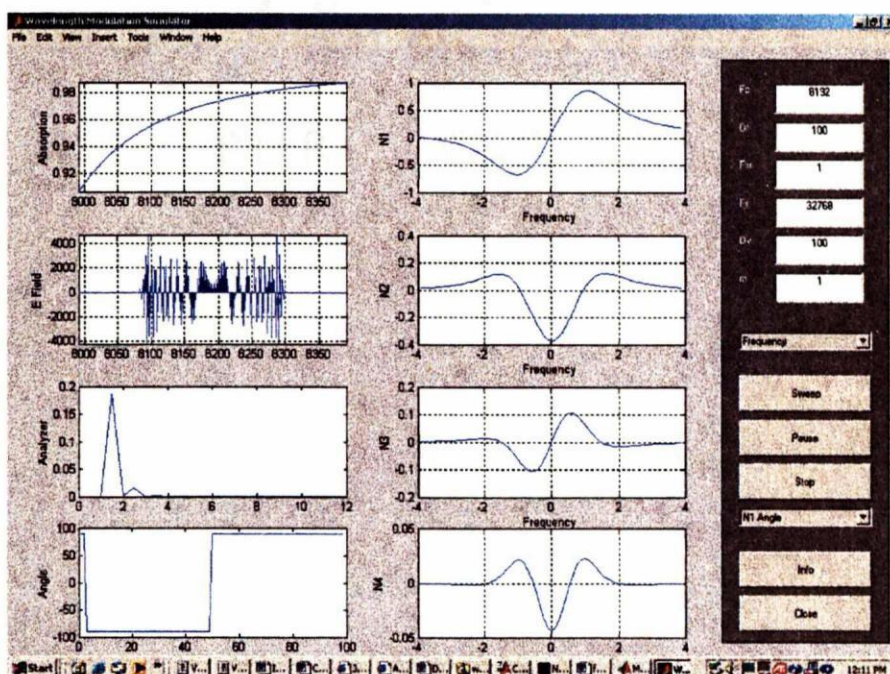


**Fig. A-1** Top left panel displays the absorption profile. The second panel on the left is the laser profile. The third panel is the Fourier Transform of the detected intensity. The bottom panel is selectable between the harmonic phase angles or the time domain signal. The right panels show the magnitudes of N1 through N4.

When the modulation index is selected, the laser is centered on the line center while the modulation index is swept. In this case, the panels on the right display the magnitudes of the even harmonics at each modulation index. A CD containing the program is included.

```
function amplitude4(action,s,ss);
%amplitude4 Demonstrates Wavelength modulation and detection.
%
```

```
global steps
```

```
steps=100;
start=0;
if nargin<1,
    action='initialize';
end;
```

```
if strcmp(action,'initialize'),
    shh = get(0,'ShowHiddenHandles');
    set(0,'ShowHiddenHandles','on')
    figNumber=figure( ...
        'Name','Wavelength Modulation Simulator', ...
        'handlevisibility','callback',...
        'IntegerHandle','on',...
        'NumberTitle','off');
```

```
%=====
```

```
% Set up the axes
```

```
frame1Hndl = axes( ...
    'Units','normalized', ...
    'Position',[0.08 0.76 0.30 0.18], ...
    'XTick',[],'YTick',[], ...
    'Box','on');
```

```
frame2Hndl = axes( ...
    'Units','normalized', ...
    'Position',[0.08 0.51 0.30 0.18], ...
    'XTick',[],'YTick',[], ...
    'Box','on');
```

```
frame3Hndl = axes( ...
    'Units','normalized', ...
    'Position',[0.08 0.26 .30 0.18], ...
    'XTick',[],'YTick',[], ...
    'Box','on');
```

```
frame4Hndl = axes( ...
    'Units','normalized', ...
    'Position',[0.08 0.03 .30 0.18], ...
    'XLim',[start steps], ...
    'XTick',[],'YTick',[], ...
```

```

    'Box','on');
frame5Hndl = axes( ...
    'Units','normalized', ...
    'Position',[0.46 0.76 0.30 0.18], ...
    'XTick',[],'YTick',[], ...
    'Box','on');
frame6Hndl = axes( ...
    'Units','normalized', ...
    'Position',[0.46 0.51 0.30 0.18], ...
    'XTick',[],'YTick',[], ...
    'Box','on');
frame7Hndl = axes( ...
    'Units','normalized', ...
    'Position',[0.46 0.26 .30 0.18], ...
    'XTick',[],'YTick',[], ...
    'Box','on');
frame8Hndl = axes( ...
    'Units','normalized', ...
    'Position',[0.46 0.03 .30 0.18], ...
    'XTick',[],'YTick',[], ...
    'Box','on');

%=====
% Information for all buttons (and menus)
labelColor=[0.8 0.8 0.8];
yInitPos=0.90;
menutop=0.95;
btnTop = 0.6;
top=0.75;
left=0.82;
btnWid=0.15;
btnHt=0.06;
textHeight = 0.05;
textWidth = 0.10;
% Spacing between the button and the next command's label
spacing=0.012;

%=====
% The CONSOLE frame
frmBorder=0.019; frmBottom=0.04;
frmHeight = 0.92; frmWidth = btnWid;
yPos=frmBottom-frmBorder;
frmPos=[left-frmBorder yPos frmWidth+2*frmBorder frmHeight+2*frmBorder];
h=uicontrol( ...
    'Style','frame', ...
    'Units','normalized', ...
    'Position',frmPos, ...
    'BackgroundColor',[0.5 0.5 0.5]);

%=====
% Carrier frequency label and text field
top = .94;
labelWidth = frmWidth-textWidth-.01;
labelBottom = top-textHeight;
labelLeft = left;

```

```

labelPos = [labelLeft labelBottom labelWidth textHeight];
h = uicontrol( ...
    'Style','text', ...
    'Units','normalized', ...
    'Position',labelPos, ...
    'HorizontalAlignment','left', ...
    'String','Fc', ...
    'Interruptible','off', ...
    'BackgroundColor',[0.5 0.5 0.5], ...
    'ForegroundColor','white');
    % Text field
textPos = [labelLeft+labelWidth labelBottom textWidth textHeight];
callbackStr = 'amplitude4("setFc")';
FcHndl = uicontrol( ...
    'Style','edit', ...
    'Units','normalized', ...
    'Position',textPos, ...
    'HorizontalAlignment','center', ...
    'Background','white', ...
    'Foreground','black', ...
    'String','8192','Userdata',8192, ...
    'callback',callbackStr);
%=====
% Change in Frequency and text field
labelBottom=top-2*textHeight-spacing;
labelLeft = left;
labelPos = [labelLeft labelBottom labelWidth textHeight];
h = uicontrol( ...
    'Style','text', ...
    'Units','normalized', ...
    'Position',labelPos, ...
    'HorizontalAlignment','left', ...
    'String','Df', ...
    'Interruptible','off', ...
    'BackgroundColor',[0.5 0.5 0.5], ...
    'ForegroundColor','white');
    % Text field
textPos = [labelLeft+labelWidth labelBottom textWidth textHeight];
callbackStr = 'amplitude4("setDf")';
DfHndl = uicontrol( ...
    'Style','edit', ...
    'Units','normalized', ...
    'Position',textPos, ...
    'HorizontalAlignment','center', ...
    'Background','white', ...
    'Foreground','black', ...
    'String','100','Userdata',100, ...
    'callback',callbackStr);
%=====
% Set Modulation frequency and text field
labelBottom=top-3*textHeight-2*spacing;
labelLeft = left;
labelPos = [labelLeft labelBottom labelWidth textHeight];
h = uicontrol( ...
    'Style','text', ...
    'Units','normalized', ...

```



```

'Position',labelPos, ...
'HorizontalAlignment','left', ...
'String','Fm', ...
'Interruptible','off', ...
'BackgroundColor',[0.5 0.5 0.5], ...
'ForegroundColor','white');
    % Text field
textPos = [labelLeft+labelWidth labelBottom textWidth textHeight];
callbackStr = 'amplitude4("setFm")';
FmHndl = uicontrol( ...
    'Style','edit', ...
    'Units','normalized', ...
    'Position',textPos, ...
    'HorizontalAlignment','center', ...
    'Background','white', ...
    'Foreground','black', ...
    'String','1','Userdata',1, ...
    'callback',callbackStr);

%=====
% Sampling frequency label and text field
labelBottom=top-4*textHeight-3*spacing;
    labelLeft = left;
labelPos = [labelLeft labelBottom labelWidth textHeight];
h = uicontrol( ...
    'Style','text', ...
    'Units','normalized', ...
    'Position',labelPos, ...
    'String','Fs', ...
    'HorizontalAlignment','left', ...
    'Interruptible','off', ...
    'Background',[0.5 0.5 0.5], ...
    'ForegroundColor','white');
    % Text field
textPos = [labelLeft+labelWidth labelBottom textWidth textHeight];
callbackStr = 'amplitude4("setFs")';
FsHndl = uicontrol( ...
    'Style','edit', ...
    'Units','normalized', ...
    'Position',textPos, ...
    'HorizontalAlignment','center', ...
    'Background','white', ...
    'Foreground','black', ...
    'String','32768','Userdata',32768, ...
    'Callback',callbackStr);

%=====
% Absorption Signal
labelBottom=top-5*textHeight-4*spacing;
    labelLeft = left;
labelPos = [labelLeft labelBottom labelWidth textHeight];
h = uicontrol( ...
    'Style','text', ...
    'Units','normalized', ...
    'Position',labelPos, ...
    'String','Dv', ...

```

```

    'HorizontalAlignment','left', ...
    'Interruptible','off', ...
    'Background',[0.5 0.5 0.5], ...
    'Foreground','white');
    % Text field
    textPos = [labelLeft+labelWidth labelBottom textWidth textHeight];
    callbackStr = 'amplitude4("setDv")';
    DvHndl = uicontrol( ...
        'Style','edit', ...
        'Units','normalized', ...
        'Position',textPos, ...
        'HorizontalAlignment','center', ...
        'Background','white', ...
        'Foreground','black', ...
        'String','100','Userdata',100, ...
        'Callback',callbackStr);

%=====
% Absorption Signal
labelBottom=top-6*textHeight-5*spacing;
    labelLeft = left;
    labelPos = [labelLeft labelBottom labelWidth textHeight];
    h = uicontrol( ...
        'Style','text', ...
        'Units','normalized', ...
        'Position',labelPos, ...
        'String','m', ...
        'HorizontalAlignment','left', ...
        'Interruptible','off', ...
        'Background',[0.5 0.5 0.5], ...
        'Foreground','white');
    % Text field
    textPos = [labelLeft+labelWidth labelBottom textWidth textHeight];
    callbackStr = 'simulat4("modulate")';
    MHndl = uicontrol( ...
        'Style','edit', ...
        'Units','normalized', ...
        'Position',textPos, ...
        'HorizontalAlignment','center', ...
        'Background','white', ...
        'Foreground','black', ...
        'String','', ...
        'Callback',callbackStr);

%=====
% The Sweep Menu
menuNumber=2;
labelStr='Frequency[Linewidth];

% Generic button information
SweepHndl=uicontrol( ...
    'Style','popupmenu', ...
    'Units','normalized', ...
    'Position',[left frmBottom+6*(btnHt+spacing) btnWid btnHt], ...

```

```

'String',labelStr, ...
'Interruptible','on');

%=====
% "Pause" button
btnNumber=1;
labelStr='Pause';

% Generic button information
PauseHndl=uicontrol( ...
'Style','togglebutton', ...
'Units','normalized', ...
'Position',[left frmBottom+4*(btnHt+spacing) btnWid btnHt], ...
'String',labelStr);

%=====
% "Stop" button
btnNumber=1;
labelStr='Stop';

% Generic button information
StopHndl=uicontrol( ...
'Style','togglebutton', ...
'Units','normalized', ...
'Position',[left frmBottom+3*(btnHt+spacing) btnWid btnHt], ...
'String',labelStr);

%=====
% "Sweep" button
btnNumber=2;
labelStr='Sweep';
callbackStr='amplitude4("sweep");';

% Generic button information
SweepHndl=uicontrol( ...
'Style','pushbutton', ...
'Units','normalized', ...
'Position',[left frmBottom+5*(btnHt+spacing) btnWid btnHt], ...
'String',labelStr, ...
'Callback',callbackStr);

%=====
% The Angle Menu
menuNumber=1;

labelStr='N1 Angle|N2 Angle|N3 Angle|N4 Angle|Time Domain';

% Generic button information
anglHndl=uicontrol( ...
'Style','popupmenu', ...
'Units','normalized', ...
'Position',[left frmBottom+2*(btnHt+spacing) btnWid btnHt], ...
'String',labelStr, ...
'Interruptible','on');

```

```

%=====
% Message box in center of figure - usually invisible
messageHndl = uicontrol('style','edit',...
    'string','Resampling speech waveform ...',...
    'units','normalized',...
    'position',[.15 .45 .5 .15],...
    'max',2,...
    'visible','off');

%=====
% The INFO button
labelStr='Info';
callbackStr='amplitude4("info")';
helpHndl=uicontrol( ...
    'Style','pushbutton', ...
    'Units','normalized', ...
    'Position',[left frmBottom+btnHt+spacing btnWid btnHt], ...
    'String',labelStr, ...
    'Callback',callbackStr);

%=====
% The CLOSE button
labelStr='Close';
callbackStr='close(gcf)';
closeHndl=uicontrol( ...
    'Style','pushbutton', ...
    'Units','normalized', ...
    'Position',[left frmBottom btnWid btnHt], ...
    'String',labelStr, ...
    'Callback',callbackStr);

hndlList=[frame1Hndl frame2Hndl frame3Hndl ...
    FcHndl FsHndl ...
    messageHndl helpHndl closeHndl DfHndl FmHndl ...
    DvHndl, frame4Hndl, frame5Hndl, frame6Hndl, frame7Hndl, frame8Hndl, PauseHndl ...
    anglHndl, MHndl, SweepHndl, StopHndl];
set(figNumber, ...
    'Visible','on', ...
    'UserData',hndlList);

set(gcf,'Pointer','watch');
drawnow
amplitude4('modulate')
set(gcf,'Pointer','arrow');
set(0,'ShowHiddenHandles',shh)
return

elseif strcmp(action,'setFc'),
    hndlList=get(gcf,'UserData');
    filtHndl = hndlList(5);
    v = get(gcf,'UserData');
    s = get(gcf,'String');
    vv = eval(s,num2str(v));
    Fs = get(filtHndl,'UserData');
    if vv>Fs/2 | vv<0, vv = v; end
    vv = round(vv);

```



```

set(gcf,'Userdata',vv,'String',num2str(vv))
amplitude4('modulate')
return

```

```

elseif strcmp(action,'setDf'),
    hndlList=get(gcf,'Userdata');
    v = get(gcf,'Userdata');
    s = get(gcf,'String');
    vv = eval(s,num2str(v));
    if vv<=0, vv = v; end
    vv = round(vv*10)/10;
    set(gcf,'Userdata',vv,'String',num2str(vv))
    amplitude4('modulate')
    return

```

```

elseif strcmp(action,'setDv'),
    hndlList=get(gcf,'Userdata');
    v = get(gcf,'Userdata');
    s = get(gcf,'String');
    vv = eval(s,num2str(v));
    if vv<=0, vv = v; end
    vv = round(vv*10)/10;
    set(gcf,'Userdata',vv,'String',num2str(vv))
    amplitude4('modulate')
    return

```

```

elseif strcmp(action,'setFm'),
    hndlList=get(gcf,'Userdata');
    v = get(gcf,'Userdata');
    s = get(gcf,'String');
    vv = eval(s,num2str(v));
    if vv<=0, vv = v; end
    vv = round(vv*10)/10;
    set(gcf,'Userdata',vv,'String',num2str(vv))
    amplitude4('modulate')
    return

```

```

elseif strcmp(action,'setFs'),
    set(gcf,'Pointer','watch');
    v = get(gcf,'Userdata');
    s = get(gcf,'String');
    vv = eval(s,num2str(v));
    if vv<=0, vv = v; end
    vv = round(vv*10)/10;
    set(gcf,'Userdata',vv,'String',num2str(vv))

```

```

    hndlList=get(gcf,'Userdata');
    messageHndl = hndlList(6);
    amplitude4('modulate')
    return

```

```

elseif strcmp(action,'modulate'), % modulate, and update display
    set(gcf,'Pointer','watch');
    axHndl=gca;
    hndlList=get(gcf,'Userdata');

```

```

frame1Hndl = hndlList(1);
frame2Hndl = hndlList(2);
frame3Hndl = hndlList(3);
FcHndl = hndlList(4);
FsHndl = hndlList(5);
DfHndl = hndlList(9);
FmHndl = hndlList(10);
DvHndl = hndlList(11);

set(gcf,'nextplot','add')

edgecolor = get(gca,'colororder'); edgecolor = edgecolor(1,:);

Fs = get(FsHndl,'UserData'); % Sampling frequency
Fc = get(FcHndl,'UserData'); % Carrier frequency
Df = get(DfHndl,'UserData'); % Change in Frequency
Fm = get(FmHndl,'UserData'); % Modulation Frequency
dv = get(DvHndl,'UserData'); % Absorption Linewidth

FFTsamples=Fs;

%Build a signal
t = (0:1/Fs:2)';
y = sin(Fm*2*pi*t);

%Build a double sided absorption signal
ff=FFTsamples/2*(0:(1/(FFTsamples)):2);
fff=ff(1:(length(ff)-1)/2);

absorp=exp(-2*8.9*10^-23*2.7*10^15*3*10^8*lorentzmf(ff,[dv,Fc])).*exp(-2*8.9*10^-
23*2.7*10^15*3*10^8*lorentzmf(ff,[dv,FFTsamples-Fc]));

%absorp=exp(-1*lorentzmf(ff,[dv,Fc])).*exp(-1*lorentzmf(ff,[dv,FFTsamples-Fc]));
absorpDisp=absorp(1:(length(absorp)-1)/2);
axes(frame1Hndl), plot(fff,absorpDisp), grid on, ylabel('Absorption')

%Modulated Signal Generation
%kf = Df/Fs*2*pi;
y1=cos(2*pi*Fc*t + Df/Fm*y);

%y1 = (y,Fc,Fs,'fm',kf);

%Laser Signal
www=(0:FFTsamples-1)/2;
Y1 = fft(y1,2*FFTsamples);
Y2 = Y1(1:FFTsamples);
axes(frame2Hndl), plot(transpose(www),abs(Y2)/FFTsamples), grid on, ylabel('Laser')

%detection signal
eField=transpose(absorp(1:length(Y1))).*Y1;
detect1= ifft(eField, 2*FFTsamples);
detect= fft((real(detect1)).^2, 2*FFTsamples);
detect2=detect(2:14*Fm+10);
www=1/2*(2:14*Fm+10);

```

```

axes(frame3Hndl), plot(www,abs((detect2))/FFTsamples), grid on, ylabel('Detection Signal')
set(gcf,'Pointer','arrow')
return

elseif strcmp(action,'sweep'), % sweep the signal
    set(gcf,'Pointer','watch');
    axHndl=gca;
    hndlList=get(gcf,'Userdata');
    SweepHndl = hndlList(20);

    sweepSelect = get(SweepHndl,'Value'); % Sampling frequency
    if sweepSelect == 1
        amplitude4('sweepFreq')
    elseif sweepSelect == 2
        amplitude4('sweepLW')
    end
    return

elseif strcmp(action,'sweepFreq'), % sweep the signal
    set(gcf,'Pointer','watch');
    axHndl=gca;
    hndlList=get(gcf,'Userdata');

    frame1Hndl = hndlList(1);
    frame2Hndl = hndlList(2);
    frame3Hndl = hndlList(3);
    FcHndl = hndlList(4);
    FsHndl = hndlList(5);
    DfHndl = hndlList(9);
    FmHndl = hndlList(10);
    DvHndl = hndlList(11);
    frame4Hndl = hndlList(12);
    frame5Hndl = hndlList(13);
    frame6Hndl = hndlList(14);
    frame7Hndl = hndlList(15);
    frame8Hndl = hndlList(16);
    PauseHndl = hndlList(17);
    anglHndl = hndlList(18);
    MHndl = hndlList(19);
    StopHndl = hndlList(21);

    set(gcf,'nextplot','add')

    edgecolor = get(gca,'colororder'); edgecolor = edgecolor(1,:);

    Fs = get(FsHndl,'UserData'); % Sampling frequency
    Fc = get(FcHndl,'UserData'); % Carrier frequency
    Df = get(DfHndl,'UserData'); % Change in Frequency
    Fm = get(FmHndl,'UserData'); % Modulation Frequency
    dv = get(DvHndl,'UserData'); % Modulation Frequency

    %===== WMS Generation
    FFTsamples=Fs;
    t = (0:1/Fs:4/Fm)';
    y = cos(Fm*2*pi*t+0*pi/180); % Wavelength Modulation

```

```

%figure, axes, plot(y(1:2000))

www=(0:FFTsamples-1)/2;
wwwDisplay=www((Fc-2*Df)*2:(Fc+2*Df)*2);

%Show Modulation Index
set(MHndl,'String',(Df/dv));

%Sweep Variables
i=1;

%Build modulation signal
y1=cos(2*pi*Fc*t + Df/Fm*y); %Electric Field

while i<steps,
%i=steps/2; %use to look at line center
%SweepSignal= 8*dv-16*i*dv/(steps);
absSweep=Fc+8*dv/2-8*dv*i/steps;
FreqValue(i)=(Fc-absSweep)/(dv);

%Laser Signal

y1 = cos(2*pi*Fc*t + Df/Fm*y);
y10 = y1;
%if i == 4
% figure, axes, plot(y1(1:2000))
%end
%=====Amplitude Modulation=====
%y1 = ((5+3*(i/steps))+(.083)*cos(2*Fm*pi*t+pi/2)).*y1; %Amplitude Modulation -- Ramp
%y1 = (10+ (.083)*cos(2*Fm*pi*t+90*pi/180)).*y1; %Amplitude without ramp+)

Y1 = fft(y1,2*FFTsamples);
Y2 = Y1(1:FFTsamples);

%Build a double sided absorption signal
ff=FFTsamples/2*(0:(1/(FFTsamples)):2);
%absorp=1-10*lorentzmf(ff, [dv, Fc+SweepSignal])-10*lorentzmf(ff, [dv, FFTsamples-
(Fc+SweepSignal)]);
absorp=exp(-2*8.9*10^-23*2.7*10^15*3*10^8*lorentzmf(ff, [dv, absSweep])).*exp(-2*8.9*10^-
23*2.7*10^15*3*10^8*lorentzmf(ff, [dv, FFTsamples-(absSweep)]));

%Sweep Signal added to Display scales To display freq shift for visual effect
absorpDisp=absorp(((Fc-2*Df)*2):(Fc+2*Df)*2);
axes(frame1Hndl), plot(wwwDisplay, absorpDisp), grid on, ylabel('Absorption'), axis('tight')

%eField signal
eField=transpose(absorp(1:length(Y1))).*Y1;
eFieldDisplay=eField((Fc-2*Df)*2:(Fc+2*Df)*2);

axes(frame2Hndl), plot(wwwDisplay, real(eFieldDisplay)), grid on, ylabel('E Field'), axis('tight')

%detection signal
detect1= ifft(eField, 2*FFTsamples);

```



```

%time_domain=(real(detect1)).^2;
amplitude_info=((5+3*(i/steps))+2*(.083)*cos(2*Fm*pi*t+pi/2));
time_domain=amplitude_info(1:length(detect1)).*(real(detect1)).^2;
%amplitudeM=(0.169*cos(2*Fm*pi*t+92*pi/180));
%amplitudeM=amplitudeM(1:length(time_domain));
%time_domain=time_domain.*amplitudeM;
    detect=fft(time_domain, 2*FFTsamples);
detect2=detect(2:14*Fm+10);
time_domain1 = (time_domain(1:100));
%Build Arrays for display
%FreqValue(i)=(Fc-SweepSignal);
%wavelength(i)=3*10^8/FreqValue(i);

N0(i)=detect(1);
N1(i)=detect(2*Fm+1);
N2(i)=detect(4*Fm+1);
    N3(i)=detect(6*Fm+1);
    N4(i)=detect(8*Fm+1);
N5(i)=detect(10*Fm+1);

%Build an array to display angle data
%test = 1/Fs*fft(y10,2*Fs);
test_axis = transpose(1:2*Fs);
test_axisshort=test_axis(1:Fs);

phi=0;
    angle0(i)=angle(detect(1))*180/pi-phi;
    angle1(i)=angle(detect(2*Fm+1))*180/pi+phi;
angle2(i)=angle(detect(4*Fm+1))*180/pi+phi;
    angle3(i)=angle(detect(6*Fm+1))*180/pi+phi;
    angle4(i)=angle(detect(8*Fm+1))*180/pi+phi;
    angle5(i)=angle(detect(10*Fm+1))*180/pi+phi;
angleSelect = get(anglHndl,'value');
if angleSelect == 5,
    detect3 = detect(1:14*Fm+10);
    %detect3 = detect2(2:size(detect2));
    first=(ifft(detect3, 2*FFTsamples));
    test_axis = transpose(1:2*Fs);
    test_axis1=test_axis(1:Fs);
    first1=first(1:Fs);
    axes(frame4Hndl),plot((test_axis1),abs(first1)), ylabel('Time Domain');
elseif angleSelect == 1
    angleDisplay=angle1;
    axes(frame4Hndl),plot(angleDisplay), ylabel('Angle')
    elseif angleSelect == 2
    angleDisplay=angle2;
    axes(frame4Hndl),plot(angleDisplay), ylabel('Angle')
        elseif angleSelect == 3
    angleDisplay=angle3;
    axes(frame4Hndl),plot(angleDisplay), ylabel('Angle')
        elseif angleSelect == 4
    angleDisplay=angle4;
    axes(frame4Hndl),plot(angleDisplay), ylabel('Angle')
end
end

```

```

%display data
axes(frame5Hndl), plot(FreqValue,imag(N1)/FFTsamples), grid on, xlabel('Frequency'), ylabel('N1')
axes(frame6Hndl), plot(FreqValue,real(N2)/FFTsamples), grid on, xlabel('Frequency'), ylabel('N2')
axes(frame7Hndl), plot(FreqValue,imag(N3)/FFTsamples), grid on, xlabel('Frequency'), ylabel('N3')
axes(frame8Hndl), plot(FreqValue,real(N4)/FFTsamples), grid on, xlabel('Frequency'), ylabel('N4')

wwwAnalyzer=1/2*(2:14*Fm+10);
axes(frame3Hndl), plot(wwwAnalyzer,(abs(detect2))/FFTsamples), ylabel('Analyzer')

drawnow;
i=i+1;
Pause = get(PauseHndl,'Value');
if Pause==1
    pause
end
Stop = get(StopHndl,'Value');
if Stop==1
    return
end

end
set(gcf,'Pointer', 'arrow')
N1data=[real(N1);FreqValue];
N2data=[real(N2);FreqValue];
N3data=[real(N3);FreqValue];
N4data=[real(N4);FreqValue];
N5data=[real(N5);FreqValue];
dlmwrite('n1ampdata.txt',N1data,'\n')
dlmwrite('n2ampdata.txt',N2data,'\n')
dlmwrite('n3ampdata.txt',N3data,'\n')
dlmwrite('n4ampdata.txt',N4data,'\n')
dlmwrite('n5ampdata.txt',N5data,'\n')
return

elseif strcmp(action,'sweepLW'), % sweep the signal
    set(gcf,'Pointer','watch');
    axHndl=gca;
    hndlList=get(gcf,'Userdata');
    frame1Hndl = hndlList(1);
    frame2Hndl = hndlList(2);
    frame3Hndl = hndlList(3);
    FcHndl = hndlList(4);
    FsHndl = hndlList(5);
    DfHndl= hndlList(9);
    FmHndl= hndlList(10);
    DvHndl= hndlList(11);
        frame4Hndl= hndlList(12);
    frame5Hndl= hndlList(13);
    frame6Hndl= hndlList(14);
        frame7Hndl= hndlList(15);
    frame8Hndl= hndlList(16);
    PauseHndl= hndlList(17);
    anglHndl= hndlList(18);
    MHndl= hndlList(19);
    StopHndl= hndlList(21);
        set(gcf,'nextplot','add')

```

```

edgecolor = get(gca,'colororder'); edgecolor = edgecolor(1,:);

Fs = get(FsHndl,'UserData'); % Sampling frequency
Fc = get(FcHndl,'UserData'); % Carrier frequency
Df = get(DfHndl,'UserData'); % Change in Frequency
Fm = get(FmHndl,'UserData'); % Modulation Frequency
dv = get(DvHndl,'UserData'); % Linewidth

FFTsamples=Fs;
t = (0:1/Fs:2)';
y = sin(Fm*2*pi*t);
    %Sweep Variables
ff=FFTsamples/2*(0:(1/(FFTsamples)):2);
fff=ff(1:(length(ff)-1)/2);
i=1;

www=(0:FFTsamples-1)/2;
wwwDisplay=www((Fc-1.5*Df)*2:(Fc+1.5*Df)*2);

%Build a double sided absorption signal

absorp=exp(-120*lorentzmf(ff, [dv, Fc])).*exp(-120*lorentzmf(ff, [dv, FFTsamples-Fc]));
absorpDisp=absorp((Fc-1.5*Df)*2:(Fc+1.5*Df)*2);

absorpG=exp(-120*gaussabs(ff, [dv, Fc])).*exp(-120*gaussabs(ff, [dv, FFTsamples-Fc]));
absorpDispG=absorpG((Fc-1.5*Df)*2:(Fc+1.5*Df)*2);

axes(frame1Hndl), plot(wwwDisplay,absorpDisp, 'b',wwwDisplay,absorpDispG, 'g --'), grid on,
ylabel('Absorption'), axis('tight')
dlmwrite('absProf.txt',real(absorpDisp),'\n')

while i<steps,

    %Laser Signal
    %kf = (Df+i*Df/10)/Fs*2*pi;
    y1=cos(2*pi*Fc*t + (Df+i*Df/10)/Fm*y);

    %y1 = modulate(y,Fc,Fs,'fm',kf);

    Y1 = fft(y1,2*FFTsamples);
    Y2 = Y1(1:FFTsamples);
    Y1display=Y1((Fc-1.5*Df)*2:(Fc+1.5*Df)*2);

    axes(frame2Hndl), plot(wwwDisplay,(real((Y1display))), 'r'), axis('tight'),grid on, ylabel('Laser'),
    axis('tight')
    %dlmwrite('laserdata.txt',real(Y1display),'\n')

    %Lorentzian absorbed eField signal
    eField=transpose(absorp(1:length(Y1))).*Y1;
    eFieldDisplay=eField((Fc-1.5*Df)*2:(Fc+1.5*Df)*2);
    axes(frame3Hndl), plot(wwwDisplay,(real(eFieldDisplay)), 'b'), axis('tight'), grid on,
    ylabel('Lorentzian'), axis('tight')
    % dlmwrite('absorta.txt',real(eFieldDisplay),'\n')

```

```

%Gaussian absorbed eField signal
eFieldG=transpose(absorpG(1:length(Y1))).*Y1;
eFieldDisplayG=eFieldG((Fc-1.5*Df)*2:(Fc+1.5*Df)*2);
axes(frame4Hndl), plot(wwwDisplay,(real(eFieldDisplayG)), 'g'), axis('tight'), grid on,
ylabel('Gaussian'), axis('tight')

%generate square law detection signals
detect1= ifft(eField, 2*FFTsamples);
detect= fft((real(detect1)).^2, 2*FFTsamples);
detect2=detect(2:20*Fm+10);

detect1G= ifft(eFieldG, 2*FFTsamples);
detectG= fft((real(detect1G)).^2, 2*FFTsamples);
detect2G=detectG(2:20*Fm+10);

%Save data in arrays
NL2(i)=detect2(4*Fm);
NL4(i)=detect2(8*Fm);
NL6(i)=detect2(12*Fm);
NL8(i)=detect2(16*Fm);
NL10(i)=detect2(20*Fm);

NG2(i)=detect2G(4*Fm);
NG4(i)=detect2G(8*Fm);
NG6(i)=detect2G(12*Fm);
NG8(i)=detect2G(16*Fm);
NG10(i)=detect2G(20*Fm);

%Determine modulation index
MIdisplay(i)=2*(Df+i*Df/10)/(dv);

%display data

%axes(frame4Hndl), plot(MIdisplay,abs((NL2))/FFTsamples), grid on, ylabel('N2')
axes(frame5Hndl), plot(MIdisplay,abs((NL2))/FFTsamples, 'b',MIdisplay,abs((NG2))/FFTsamples, 'g'
), grid on, ylabel('N2')
axes(frame6Hndl), plot(MIdisplay,abs((NL4))/FFTsamples, 'b',MIdisplay,abs((NG4))/FFTsamples, 'g'
), grid on, ylabel('N4')
axes(frame7Hndl), plot(MIdisplay,abs((NL6))/FFTsamples, 'b',MIdisplay,abs((NG6))/FFTsamples, 'g'
),grid on, ylabel('N6')
axes(frame8Hndl), plot(MIdisplay,abs((NL8))/FFTsamples, 'b',MIdisplay,abs((NG8))/FFTsamples, 'g'
), grid on, ylabel('N8')

www=1/2*(2:20*Fm+10);
%axes(frame3Hndl), plot(www,abs((detect2))/FFTsamples)
set(DfHndl,'String',(Df+i*Df/10));
set(MHndl,'String',(2*(Df+i*Df/10)/(dv)));

drawnow;
i=i+1;
Pause = get(PauseHndl,'Value');

```



```

    if Pause==1
        pause
    end
    Stop = get(StopHndl,'Value');
    if Stop==1
        return
    end

end
set(gcf,'Pointer', 'arrow')
return

elseif strcmp(action,'info'),
    set(gcf,'pointer','arrow')
        ttlStr = get(gcf,'Name');
        hlpStr1 = [...
            'Runs well '
        ];

        hlpStr2 = [...
            '];
        hlpStr3 = [...
            '];

myFig = gcf;
helpfun(ttlStr,hlpStr1,hlpStr2,hlpStr3);
return % avoid fancy, self-modifying code which
% is killing the callback to this window's close button
% if you press the info button more than once.
% Also, a bug on Windows MATLAB is killing the
% callback if you hit the info button even once!

% Protect against(gcf changing -- Change close button behind
% helpfun's back
ch = get(gcf,'ch');
for i=1:length(ch),
    if strcmp(get(ch(i),'type'),'uicontrol'),
        if strcmp(lower(get(ch(i),'String')),'close'),
            callbackStr = [get(ch(i),'callback') ...
                '; amplitude4("closehelp",' num2str(myFig) ')];
            set(ch(i),'callback',callbackStr)
        end
    end
end
return

elseif strcmp(action,'closehelp'),
    % Restore close button help behind helpfun's back
    ch = get(gcf,'ch');
    for i=1:length(ch),
        if strcmp(get(ch(i),'type'),'uicontrol'),
            if strcmp(lower(get(ch(i),'String')),'close'),
                callbackStr = get(ch(i),'callback');
                k = findstr('; amplitude4(',callbackStr);

```

```
callbackStr = callbackStr(1:k-1);  
set(ch(i),'callback',callbackStr)  
break;  
end  
end  
end  
ch = get(0,'ch');  
if ~isempty(find(ch==s)), figure(s), end % Make sure figure exists  
end
```

**VITA**  
**for**  
**James M. Barrington**

**DEGREES:**

Bachelor of Science (Computer Engineering), Old Dominion University, Norfolk, VA  
May 2000  
Master of Science (Electrical Engineering), Old Dominion University, Norfolk, VA  
May 2002

**PROFESSIONAL CHRONOLOGY:**

Old Dominion University, Norfolk, Virginia  
June 1998 - Present

Submarine Training Facility, Norfolk, Virginia  
Curriculum and Instructional Standards Officer, October 1994 – May 1998

Submarine Squadron Eight, Norfolk, Virginia  
Sonar Officer, July 1991 – September 1994

USS Oklahoma City (SSN 723), Norfolk, Virginia  
Sonar Leading Chief Petty Officer, January 1986 – June 1991

Fleet Antisubmarine Warfare Training Center, San Diego, California  
Instructor, November 1981 – December 1985

USS Francis Scott Key (SSBN 657B), Charleston, South Carolina  
Sonar Supervisor, May 1977 – October 1981

**SCIENTIFIC AND PROFESSIONAL SOCIETIES MEMBERSHIP:**

Institute of Electrical and Electronics Engineers (IEEE) Student Member  
Tau Beta Pi  
Etta Kappa Nu

**HONORS AND AWARDS:**

Computer Engineering Faculty Award 2000

**GRANTS AWARDED:**

Virginia Space Consortium Undergraduate Research Grant  
Graduate Assistance in Areas of National Need (GAANN) Doctoral Fellowship

**SCHOLARLY PUBLICATIONS:**

A. M. Khan, J. M. Barrington and A. N. Dharamsi, "Sensitive Detection of Molecular Species by Modulation Techniques: A Quantitative Measure of the Information Content in Spectroscopy," Methods of Ultrasensitive Detection, II; Vol. 4634 pp 83-91, 2002 (Photonics West, LSAE2002, Symposium LA06, Conference 4634), January 21, 2002 San Jose, CA

J.M. Barrington, A.M. Bullock and A.N. Dharamsi "Precise absorption line feature measurements with higher harmonic detection," 2001 Conference on Lasers and Electro-Optics, Baltimore, MD. Conference Sponsored by IEEE Lasers and Electrooptic Society, Optical Society of America, Quantum Electronics Division of the European Physical Society Optical Society Japanese Quantum Electronics Joint Group, Paper CThG, Thursday May 10, 2001, Technical Digest pp 407-409.

A.M. Bullock, J.M. Barrington, and A. N. Dharamsi, "Sensitive Non-intrusive Sensing by Modulation Spectroscopy with Diode Lasers," Photonics West, San Jose, January 2001 Conference 4285A January 2001 Proceedings of SPIE Vol. 4285A Laser Diodes and LEDs in Industrial, Measurement, Imaging and Sensor Applications III- Paper Number [4285A-08]